Unifying in vitro and in vivo IVT mRNA expression discrepancies in skeletal muscle via mechanotransduction

Sushma M. Bhosle, Kristin H Loomis, Jonathan L Kirschman, Emmeline L Blanchard, Daryll Vanover, Chiara Zurla, Damien Habrant, Darin Edwards, Patrick Baumhof, Bruno Pitard, et al.

Accepted Manuscript

Unifying *in vitro* and *in vivo* IVT mRNA expression discrepancies in skeletal muscle via mechanotransduction

Sushma M. Bhosle, Kristin H. Loomis, Jonathan L. Kirschman, Emmeline L. Blanchard, Daryll A. Vanover, Chiara Zurla, Damien Habrant, Darin Edwards, Patrick Baumhof, Bruno Pitard, Philip J. Santangelo

PII: S0142-9612(18)30016-4

DOI: 10.1016/j.biomaterials.2018.01.010

Reference: JBMT 18425

To appear in: *Biomaterials*

Received Date: 29 June 2017

Revised Date: 30 December 2017

Accepted Date: 6 January 2018

Please cite this article as: Bhosle SM, Loomis KH, Kirschman JL, Blanchard EL, Vanover DA, Zurla C, Habrant D, Edwards D, Baumhof P, Pitard B, Santangelo PJ, Unifying *in vitro* and *in vivo* IVT mRNA expression discrepancies in skeletal muscle via mechanotransduction, *Biomaterials* (2018), doi: 10.1016/j.biomaterials.2018.01.010.

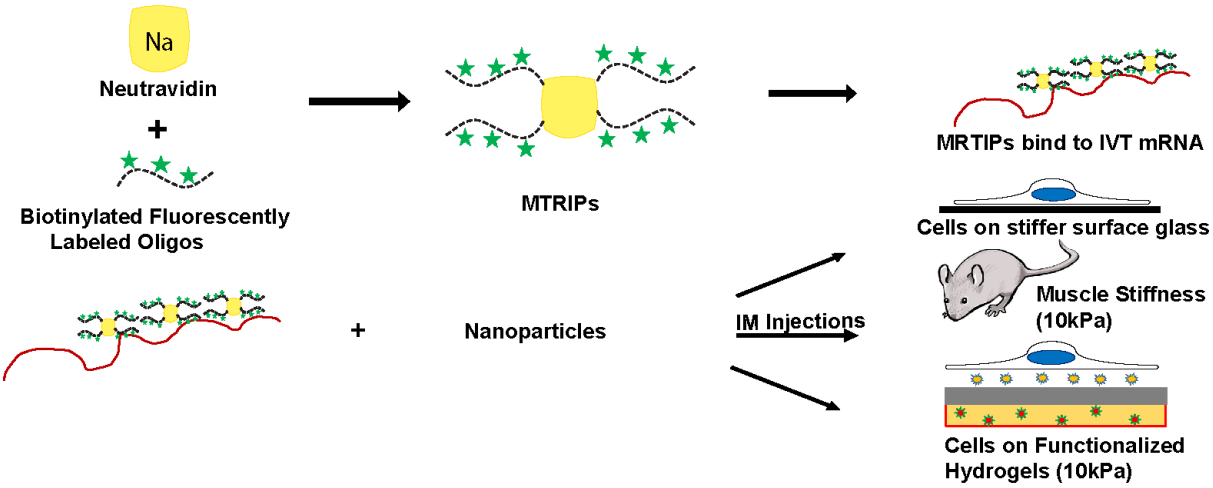

Unifying *in vitro* and *in vivo* IVT mRNA expression discrepancies in skeletal muscle via mechanotransduction

Sushma M. Bhosle [a], Kristin H. Loomis [a], Jonathan L. Kirschman [a], Emmeline L. Blanchard [a], Daryll A. Vanover [a], Chiara Zurla [a], Damien Habrant [b], Darin Edwards [c], Patrick Baumhof [d], Bruno Pitard [b]*, and Philip J. Santangelo [a]*

[a]Wallace H. Coulter Department of Biomedical Engineering, Georgia Institute of Technology and Emory University, 950 Atlantic Dr. NW, Engineered Biosystems Building, Atlanta, GA, 30332, USA
[b]In-Cell-Art, 21 rue de la Noue Bras de Fer, 44200 Nantes, France
[c]Sanofi Pasteur, VaxDesign Corporation, 2501 Discovery Dr Suite 300, Orlando, FL 32826
[d]CureVac AG, Paul-Ehrlich-Str. 15, 72076 Tübingen, Germany
* To whom correspondence should be addressed.

Dr. Philip J. Santangelo
Email: philip.santangelo@bme.gatech.edu,
Tel: 404-385-2116; Fax: 404-894-4243.

Dr. Bruno Pitard,
Email : bruno.pitard@incellart.com,
Tel : (33) (0)6 73 19 12 02.

Abstract

The translational efficiency of an *in vitro* transcribed (IVT) mRNA was measured upon delivery to primary skeletal muscle cells and to a mouse model system, towards the development of a predictive *in vitro* assay for the screening and validation of intramuscular mRNA-based vaccines. When IVT mRNA was delivered either naked or complexed with novel aminoglycoside-based delivery vehicles, significant differences in protein expression *in vitro* and *in vivo* were observed. We hypothesized that this previously anticipated discrepancy was due to differences in the mechanism of IVT mRNA endosomal entry and release following delivery. To address this, IVT mRNA was fluorescently labeled prior to delivery, to visualize its distribution. Colocalization with endosomal markers indicated that different entry pathways were utilized *in vivo* and *in vitro*, depending on the delivery vehicle, resulting in variations in protein expression levels. Since extracellular matrix stiffness (ECM) influences mRNA entry, trafficking and release, the effect of mechanotransduction on mRNA expression was investigated *in vitro* upon delivery of IVT mRNA alone, and complexed with delivery vehicles to skeletal muscle cells grown on ~10kPa hydrogels. This *in vitro* hydrogel model more accurately recapitulated the results obtained *in vivo* upon IM injection, indicating that this approach may assist in the characterization of mRNA based vaccines.

Key Words: Skeletal Muscle cells; mRNA delivery; Hydrogels; ECM protein; Mechanotransduction; Nanoparticles.

Abbreviated Title: Mechanotransduction explains IVT mRNA expression differences *in vitro* and *in vivo*.

1. Introduction

Since their early development, messenger RNA based vaccines have demonstrated their potential application in a wide variety of animal models as well as in humans [1,2,3]. For intra-muscular administration, a formulation that stabilizes the mRNA-based vaccine against RNAse-mediated degradation, while promoting efficient cellular uptake, is beneficial.

Cationic lipid nanoparticles have been widely utilized for delivering nucleic acids, as they are rapidly internalized due to their surface charge as well as their ability to disrupt the endosomal membrane to facilitate cargo release in to the cytosol [4,5]. They have also been successfully utilized in topical gene delivery, due to their surface charge interaction with the skin [6]. Although cationic lipid particles are efficiently expressed *in vitro*, little success has been achieved *in vivo* [7,8]. On the contrary, naked synthetic *in vitro* transcribed (IVT) mRNA injected intramuscularly is expressed *in vivo* in mice but not *in vitro* [9,10]. These discrepancies between *in vivo* and *in vitro* transfection efficiencies are not surprising, since it has been previously reported in experiments performed with nucleic acids complexed with different delivery vehicles. The results of such experiments, summarized in Table 1, further complicate our understanding of the mechanisms underlying successful delivery of nucleic acids-based therapeutics. This highlights the importance of novel approaches that allow for high-throughput screening of nanocarriers *in vitro* toward the development of vaccine formulations, prior to *in vivo* studies.

IVT mRNA often enter cells by receptor-mediated endocytosis, followed by uptake into the endosomal system and degradation in lysosomes. However, a fraction of mRNAs escape from the endosomal compartment and are released into the cytosol, leading to ribonucleoprotein formation and protein expression [19]**.** The entry pathways for lipid and polymer-based complexes depend on the cell type, expression of specific endocytic markers and charge of the nanocomplexes. For example, muscle and endothelial cells, fibroblasts, and adipocytes express high amounts of caveolin, and therefore caveolin-mediated entry prevails [20,21]. Differences in entry pathways are also observed between different delivery vehicles. For example, lipoplexes are internalized by clathrin-mediated endocytosis, and are expressed efficiently, whereas polyplexes are internalized by caveolae or by both clathrin and caveolin-dependent endocytosis, which leads to decreased expression efficiency [22,23].

Recently, easily dispersible and porous antibiotics-conjugated nanoparticles have been utilized to produce formulations for treating lung infection [24]. Kanamycin, an aminoglycoside antibiotic, potentiates the antibacterial effect of gold nanoparticles [25], therefore, kanamycin-capped gold particles were produced through a simple, biofriendly reaction to yield stable and monodispersed particles. These lipidic aminoglycoside derivatives are known to deliver siRNA and yield efficient gene silencing [26] as well as other nucleic acids [27,28].

Here, bio-inspired ionizable lipids, containing an aminoglycoside cationic head group Kanamycin and bearing a cholesterol moiety as the hydrophobic part were synthesized. The resulting molecules were termed CholK (Cholesterol-Kanamycin) and DosK (DioleylSuccinyl-Kanamycine). We utilized CholK and DosK as delivery vehicles to measure the efficiency of transfection of IVT mRNA *in vitro* and *in vivo*, in order to understand the mechanism underlying the experimental discrepancies previously described.

We hypothesized, first of all, that the differences in protein production *in vivo* and *in vitro* might depend on the endocytic pathway utilized for entry. Therefore, we investigated the endocytic pathway of naked IVT mRNA or complexed with aminoglycoside lipidic derivatives, CholK and DosK, their release from the endosomal system, and protein expression *in vitro*, in human skeletal muscle cells, and *in vivo*, in a mouse model.

IVT mRNA was fluorescently labeled, prior to delivery, with the single-molecule-sensitive probes MTRIPs (multiply-labeled tetravalent RNA imaging probes) to assess its cellular localization with respect to the endocytic compartment. The RNA imaging strategy, composition and delivery of MTRIPs to living cells (Fig. S1) has been comprehensively described in Santangelo et al [29,30]. Briefly, MTRIPs are fluorescently labeled tetravalent single RNA sensitive probes consisting of a neutravidin core and four biotinylated fluorescently labeled 2'OMe-RNA oligonucleotides for specific mRNA targeting. This chemistry ensures an optimal level of affinity to bind target mRNAs without inhibiting translation, without the toxicity observed for other chemical modifications and without triggering a cellular immune response. To date, MTRIPs have been successfully utilized to study endogenous and plasmid-derived mRNAs such as β-actin, c-myc and poly(A) transcripts, and

the interaction with regulatory proteins and RNA granules in fixed and living cells via both colocalization analysis and proximity ligation assays (PLA) [31,32,33,34,35,36]. MTRIPs were also utilized to study the RSV genome, its organization in viral particles, its localization in infected cells and interactions with viral and host cells [37,38]. Recently, we applied this single RNA sensitive probes to visualize synthetic mRNA uptake *in vitro* and in *ex vivo* tissue sections, as well as to characterize the release kinetics from endocytic compartments, and mRNA-protein expression correlations [39].

To directly measure translation efficiency, an IVT mRNA encoding for the firefly luciferase was used as a model system. Our results indicated that IVT mRNA transfected with DosK was endocytosed prevalently by a caveolin-dependent pathway and was expressed efficiently *in vitro,* but not *in vivo*. On the contrary, naked IVT mRNA or complexed with CholK was endocytosed predominantly via a clathrin-dependent pathway and was expressed *in vivo,* but not *in vitro*.

To develop an *in vitro*, high-throughput assay that would allow for the accurate prediction *in vitro*, of the outcome of *in vivo* experiments, we first investigated the role of two individual ECM proteins, fibronectin and collagen, which are among the most abundant and extensively characterized in the context of nucleic acids delivery *in vitro*. Specifically, fibronectin and collagen were previously utilized to study the uptake mechanism and transfection efficiencies of polyplexes in mesenchymal stem cells (MSCs), NIH/3T3 and PC12 cells, and compared to laminin, polylysine and BSA [40,41,42]. For example, gene transfer was shown to be enhanced in NIH/3T3 cells plated on fibronectin, whereas collagen IV improved transfection in PC12 cells [43,44]. Here, addition of an excess of either fibronectin or collagen led to a switch in the endosomal entry pathway from caveolin to clathrin- mediated endocytosis, without altering protein production upon delivery of either naked IVT mRNA or complexed with CholK. Therefore, this strategy failed to accurately recapitulate the results obtained *in vivo,* addressing the need for further investigation.

We hypothesized that the differences in protein production *in vivo* and *in vitro* might be a consequence of a variation in substrate stiffness, which exerts varied mechanical cues attributing to the observed *in vivo* and *in vitro* discrepancies. The mechanical properties of cellular microenvironment transmit biochemical cues that alter cellular functions including motility, adhesion, proliferation, migration, apoptosis, and differentiation [45,46,47,48]. Moreover, the mechanical cues generated by physical forces like tension, compression and shear stress, and alteration in the mechanical forces by ECM directly or indirectly regulate transcriptional regulation, contributing to pluripotency, self-renewal and differentiation in embryonic and stem cells [49]. For example, matrix stiffness influences mesenchymal stem cell differentiation [50], modulates gene uptake and regulates the dissociation of pDNA from the condensation agent and eventually affects pDNA expression [51]. ECM protein crosslinking and stiffening leads to progression of tumors in breast cancer via integrin signaling [52]. The transfection efficiency of polyplexes is highly enhanced by matrix stiffness [53,54,55].

Studies on biomaterials in tissue engineering indicated that hydrogels have the ability to generate physiologically relevant biomaterial *in vitro.* For example, hydrogels have been used to culture human embryonic stem cells (hES) [56,57]. Moreover, hydrogels with tunable stiffness have been used to study the regulation of differentiation in liver stem cells and hepatocytes [58] and during osteogenic differentiation of human mesenchymal cells [50].

Here, we utilized polyacrylamide (PA) hydrogels with stiffness of ~10 kPa [59,60] as a model to mimic ECM stiffness in muscle and studied the differences in the uptake, endosomal entry, release and protein expression of naked IVT mRNA or complexed with aminoglycoside lipidic derivatives in skeletal muscle cells. This approach more accurately recapitulated evidence obtained *in vivo* upon IM injection. Our results indicated that cells cultured on hydrogel significantly overexpressed genes involved in mRNA translation, suggesting how mechanical forces applied to cells may influence the activation of mRNA translational pathways.

2. Materials and methods

2.1. mRNA synthesis

In brief, linearized plasmid harboring the sequence of luciferase downstream of a T7 promoter was transcribed using T7 RNA polymerase (Thermo Scientific, Braunschweig, Germany). mRNA vectors contained a 5′ cap structure, 5′ UTR, open reading frame, 3′ UTR and polyA tail. They were sequence optimized and did not include chemically modified nucleotides [1]. The mRNA was produced by T7-polymerase-based *in vitro* run-off transcription. IVT mRNAs were purified according to the same protocol by reversed-phase chromatography using a PLRP-S stationary phase and an acetonitrile gradient in a triethylammonium acetate buffer. A detailed protocol has been described elsewhere [61].

2.2. Zeta potential of mRNA / Kanamycin lipidic derivatives complex

IVT Luciferase mRNA was provided by CureVac AG (Tübingen, Germany) and the delivery vehicles were provided by In Cell Art (Nantes, France). CholK was used at mRNA:CholK charge ratio of 0.1 and DosK at a charge ratio of 5. The particle size and zeta potential of the nanoparticles was measured with a Zetasizer Nano ZS (Malvern Instruments). The nanoparticles were diluted in either PBS to measure size or in deionized water to measure the zeta potential.

2.3. Cell Line and Transfections

Hela and A549 cell line (ATCC) were cultured in DMEM (Lonza) supplemented with 10 % FBS (Hyclone), and 100 U/mL penicillin and 100 µg/ml streptomycin (Life Technologies), for the characterization of IVT mRNA labeled with MTRIPS transfected with Lipofectamine 2000 (following the manufacturer's protocol). Primary human skeletal muscle cells, HSkMSC, (PromoCell) were grown in HSkMSC growth media (PromoCell) supplemented with growth factors, penicillin and streptomycin. Cells were plated the day prior to transfections with MTRIPs labeled or unlabeled firefly luciferase IVT mRNA, either naked or complexed with the delivery vehicles. For growth and differentiation of human skeletal muscle cells, the cells were cultured in skeletal muscle cell growth medium until they reach approximately 60 – 80 % confluence and then the medium was replaced with skeletal muscle cell differentiation medium (PromoCell). Cells were cultured for 5-6 days and media replaced every 2-4 day. Myotubes were switched back to HSkMSC growth media and used for transfections. Sol8 (ATCC) mouse skeletal muscle cells were cultured in DMEM (Lonza) supplemented with 20 % FBS, penicillin and streptomycin.

mRNA and CholK solutions were prepared in Ringers Lactate, RiLa (Bio scientific) in separate tubes in a final volume of 50 µl for experiments in Labtek II and in 250 µl for experiments in 6 well plates. The mRNA and CholK solutions were then mixed and incubated for 15 min. Similarly, mRNA and DosK solutions were prepared separately in RiLa in a final volume of 25 µl for experiments in Labtek II (Nunc) and in 100 µl of RiLa for experiments in 6 well plates. 500 ng RNA were used to transfect cells in Labtek II (Nunc) while 8 µg were used to transfect cells plated on 25 mm cover glass (Fisher) in 6 well plates. Cells were washed with Ca/Mg free PBS. Naked mRNA or complexed with CholK in RiLa solution were added to the cells for 10 min, followed by addition of fresh media. mRNA complexed with DosK was instead added to cells in media. Media was replaced after 4 h for all conditions. Cells were fixed and stained for endosomal markers 1.5 h or 6 h post-delivery or lysed for luciferase expression detection 24 h post-delivery. To study mRNA endocytic pathway and protein production in presence of ECM proteins, Labtek II were coated with Fibronectin (Sigma) at 100 µM and collagen (Stem Cell Technologies) at 100 µM overnight at 4^{o} C, followed by incubation at 37^{o} C overnight before mRNA transfection [40]. Cells were pre-incubated for 30 min in Chlorpromazine, a clathrin inhibitor (Alfa Aesar) at the concentration of 10 µg/ml and genestein, a caveolin inhibitor (TSZ Chem) at the concentration of 100 µM.

2.4. Preparation of CholK and DosK.

The nanoparticles were prepared in five steps starting from Kanamycin A, according to the schematic described in S1 and the procedures described below adapted from Sainlos et al [62]. *Kanamycin-Cbz-Teoc$_3$ 3:* Kanamycin A (1.15 g, 2.38 mmol, 1 eq.) was dissolved in water (10 mL). Et_3N (0.33 mL, 2.38 mmol, 1 eq.) and a solution of *N*-benzyloxycarbonyloxy-5-norbornene-2, 3-dicarboximide (744 mg, 2.38 mmol, 1 eq.) in DMF (15 mL) were successively added and the mixture was stirred at room temperature (RT) for 24 h. A solution of 2-(trimethylsilyl)ethyl-4-nitrophenylcarbonate (2.30 g, 9.76 mmol, 4.1 eq.) in DMF (20 mL) and more Et_3N (1.36 mL, 9.76 mmol, 4.1 eq.) were then added and the yellow solution was stirred at 55° C for 48 hours. The mixture was then concentrated and the residue taken up with EtOAc, before washing with NaOH 1M (3 times), water and brine. The organic fraction was dried over $MgSO_4$ and concentrated *in vacuo*. The residue was purified by flash chromatography (DCM/MeOH) to afford the expected product (1.22 g, 49 %). ^{1}H NMR (MeOD, 25°C), 0.02-0.05 (m, 27H), 0.98-1.02 (m, 6H), 1.50- 1.53 (m, 1H), 2.04-2.08 (m, 1H), 3.19 (t, J=9.4 Hz, 1H), 3.41-3.75 (m, 14H), 4.11-4.16 (m, 7H), 5.03-5.10 (m, 4H), 7.29-7.38 (m, 5H); MS (ESI+) 1074.5 $[M+Na]^+$.
Kanamycin-Teoc$_3$ 4: To a solution of *Kanamycin-Cbz-Teoc$_3$* (1.3 g, 1.23 mmol, 1 eq.) in degassed wet MeOH (containing 10 % of H_2O, 50 mL) was added 10 % Pd/C (0.17 g, 0.1 eq.). 3 cycles of vacuum/N_2 were applied, followed by 3 cycles of vacuum/H_2. The mixture was stirred overnight, then filtered over a pad of cellite and washed with EtOH. The filtrate was concentrated *in vacuo* and the residue purified by flash chromatography (DCM/MeOH) to afford the expected free amine (0.671 g, 59 %). ^{1}H NMR (MeOD, 25°C), 0.00-0.02 (m, 27H), 0.93-0.95 (m, 6H), 1.46-1.52 (m, 1H), 1.98-2.07 (m, 1H), 2.59-2.64 (m, 1H), 2.92-2.96 (m, 1H), 3.04-3.09 (t, J=9.3 Hz, 1H) 3.32-3.57 (m, 4H), 3.60-3.69 (m, 9H), 4.03-4.13 (m, 7H), 5.01 (s, 2H), 5.12 (s, 1H); MS (ESI+) 939.6 $[M+Na]^+$.
(Cholesteryloxy-3-carbonyl)]Kanamycin-Teoc$_3$ 5: Et_3N (0.12 mL, (1.5 mL, 0.87 mmol, 1.2 eq.) and cholesteryl chloroformate (0.330 g, 0.73 mmol, 1 eq.) were added to a solution of *Kanamycin-Teoc$_3$* (0.670 g, 0.73 mmol, 1 eq.) in THF (70 mL) and DMF (15 mL). The mixture was stirred at RT overnight, then concentrated *in vacuo*. The residue was purified by flash chromatography (DCM/MeOH) to afford the expected product (0.655 g, 67 %). ^{1}H NMR (MeOD, 25° C), 0.00-0.02 (m, 27H), 0.67 (s, 3H), 0.82-1.59 (m, 39H), 1.84-2.02 (m, 6H), 2.27-2.29 (m, 2H), 3.07-3.09 (m, 1H), 3.33-3.39 (m, 6H), 3.53-3.69 (m, 9H), 3.86-3.89 (m, 1H), 4.02-4-11 (m, 6H), 4.55 (s, 1H), 5.01-5.01 (m, 2H), 5.34 (s, 1H); MS (ESI+) 1352.0 $[M+Na]^+$.
CholK: To a suspension of *(Cholesteryloxy-3-carbonyl)]Kanamycin-Teoc$_3$* (0.650 g, 0.49 mmol) in DCM (6 mL) was slowly added TFA (12 mL) at 0°C. The solution was stirred at RT for 2 h and then concentrated. After 3 consecutive additions of MeOH and subsequent evaporations, the residue was purified by flash chromatography (reverse phase, C18-Silica, H_2O+0.05 %TFA/MeOH) and lyophilized to give CholK (0.370 g, 61 %). ^{1}H NMR (MeOD, 25° C), 0.72 (s, 3H), 0.87-63 (m, 34H) , 1.85-2.07 (m, 6H), 2.32-2.34 (m, 2H), 2.45-2.55 (m, 1H), 3.17-3.19 (m, 1H), 3.35-3.88 (m, 15H), 4.30-4.50 (m, 1H), 5.10 (s, 1H), 5.26 (s, 1H), 5.38 (s, 1H). MS (ESI+) 919.4 $[M+Na]^+$.
DosK was prepared starting from *Kanamycin-Teoc$_3$ 4* then linked to 4-(Dioleylamino)-4-oxobutanoic Acid to produce *N,N Dioleyl-succinamide-Kanamycin-Teoc$_3$* followed by Teoc deprotection and purification, according to procedures extensively described in [27,28,63].

2.5. Labeling of Luciferase IVT mRNA

The synthesis of fluorescently labelled MTRIPs been previously described [29]. Briefly, MTRIPs consist of 15-17 nucleotide long 2' O-methyl RNA-DNA chimeric oligonucleotides, containing three to four amino-modified thymidines, a short poly(T) linker and a 5' biotin (Biosearch Technologies, Petaluma, CA).

Three oligonucleotides were selected for IVT mRNA labeling, complementary to 3 separate sequences in the human Albumin 3' UTR of the reporter Luciferase mRNA (Table 2). Oligonucleotides were labeled with either Cy3B-NHS ester (GE Healthcare) or Dylight 650/680-NHS esters (Pierce) using manufacturer protocols, and excess dye was removed using 3 kDa centrifugal filters (Millipore). MTRIPs were assembled by incubation

of the biotinylated and fluorescently labeled oligos with Neutravidin (Pierce) at a 5:1 ratio for 1 hour at RT followed by filtration using 30kD MWCO centrifugal filters.

For labeling with MTRIPs, IVT mRNA was buffer exchanged in 1x PBS, heated to 75^{o} C for 10 min and immediately placed on ice. MTRIPs were added at a 1:1 mRNA: MTRIP ratio, and incubation was allowed to proceed overnight at 37° C. The next day, the labeled IVT mRNA was filtered using a 200 kD MWCO ultrafiltration unit (Advantec MFS Inc) to remove unbound MTRIPs and concentrated by 30 kD MWCO centrifugal filters [39,64]

2.6. Animals and Histology

Female BALB/C mice (Charles River, Wilmington, MA), age group 6 to 8 weeks were anesthetized with 2.5% isoflurane. Mice were injected in the anterior tibialis, intramuscularly using 10 µg of IVT mRNA alone or complexed with CholK or DosK in 40 µl of RiLa using a 29G needle. The alternate leg was used as a sham injection control. Unlabeled or Dylight 680 -labeled IVT mRNA were used for luciferase mRNA expression studies, while IVT mRNA labeled with Cy3B was used to study the colocalization with endosomal markers. The anterior tibialis muscle was removed 1.5 h and 6 h post-delivery for endosomal marker staining and 16 hours post-delivery for luciferase protein expression. Tissue was fixed in 4% PFA, embedded in paraffin wax and 5-micron thick sections were obtained. Mice were housed and manipulated under specific-pathogen-free conditions in the animal care facilities of Georgia Institute of Technology. All animal handling and experiments were performed in accordance with protocols approved by the IACUC at Georgia Institute of Technology.

2.7. Luciferase Assay

Luciferase reporter expression was detected with the Bright glow^{TM} Luciferase Assay System (Promega) for all *in vitro* studies. Cells (30,000) were grown in Labtek II, transfected with RNA alone or complexed with the delivery vehicles. 24 h post-delivery, cells were washed once with PBS, lysed with glo lysis buffer, and 100 µl of luciferin substrate reagent were added, according to the manufacturer protocol. Luminescence was measured immediately in a 96 well plate reader (Biotek Synergy H4 multimode plate reader). For hydrogel experiments, cells (0.5 X 10^{6}) were plated in a 6 well plate, transfected with IVT mRNA alone or with the delivery vehicles. 24 h post-delivery, cells were trypsinized, washed with PBS, lysed with Glo lysis buffer and the bright glow substrate reagent was added. The protein concentration of the lysates was quantified with BCA assay and the luciferase reads were normalized per mg of total protein.

2.8. Immunofluorescence staining and microscopy analysis

Cells were fixed with 4 % PFA for 10 min, blocked with 5 % donkey serum and 1 % BSA, and immunostained using appropriate antibodies. The markers for the entry pathway utilized were Caveolin-1, and Clathrin Light Chain (Santa Cruz Biotechnology). The endocytic markers used were CD63 (mouse anti-CD63, Developmental studies Hybridoma Bank- DSHB), EEA1 (mouse anti-EEA1, BD Biosciences), and Rab7 (rabbit anti-Rab7, Abcam). Mouse tissue slides were stained with CD63 (Mouse anti-CD63, Santa Cruz Biotechnology), Rab5 and Rab7 (Rabbit anti-Rab5 and Rab7, Abcam). Luciferase protein was detected with a mouse anti-luciferase antibody (Santa Cruz Biotechnology). Secondary antibodies were purchased pre-conjugated to either Alexa Fluor 488 (Life Technologies), Cy3 (Jackson Immunoresearch), or Alexa Fluor 647 (Life Technologies). Secondary antibody incubation was performed for 45 min at 37^{o} C for cell lines and at RT for tissue sections. Cells were also stained with DAPI for 5 minutes and mounted on glass slides with Prolong gold.

Cells and tissue sections were imaged with a Zeiss Plan-Apo 60X 1.4 NA oil objective on an Ultra View Spinning Disk equipped with a Hamamatsu Flash 4.0v2 CMOS camera or with a Nikon Plan-Apo 60X 1.4 NA oil objective on a Nikon Eclipse TE2000 widefield microscope equipped with a Hamamatsu C9000-02 EM-CCD camera. Both microscopes were controlled by Volocity acquisition software (PerkinElmer). Where indicated, tissue sections were imaged with at Zeiss Plan-Apo 60X 1.4 NA oil objective on Zeiss Elyra PS.1/ 780 super resolution microscope.

Colocalization of IVT mRNA with endosomal markers was quantified using the Mander's correlation coefficient for 15 cells per condition using Volocity software. The quantification of the percentage of cytosolic free mRNA and trapped in the endosomal system was performed using Volocity software as follows. All mRNAs were identified as "objects", sorted based on their size (either <1 µm or > 1 µm) and fluorescence intensity (above background), and colocalization with endocytic markers was measured. mRNA granules with size > 1 µm either colocalized with endocytic markers or were found outside the cells, as verified by visual inspection. mRNA granules <1 µm were considered to be cytosolic if they did not overlap or touch endosomal markers. For each cell, the sum of cytosolic free mRNA and mRNA trapped in endosomes was recorded and plotted using Sigmaplot. At least 15 cells were used per condition in all experiments.

2.9. Immunohistochemical Staining

Tissue section slides were deparaffinized and incubated in antigen retrieval buffer (Dako, Carpinteria, CA) for 20 min on steam followed by cooling at RT for 20 min. The slides were washed with TBS with 0.1 % tween-20 (CalBioChem), with TBST for 5 min twice and blocked with TBST containing 5 % donkey serum and 1 % BSA for 1 h, and finally incubated with luciferase antibody (Goat anti-luciferase, Promega) overnight at 4^{o} C. Next, the slides were washed three times with TBST and incubated with 3 % Hydrogen peroxide in PBS for 15 min to quench the endogenous peroxidase activity. The slides were washed three times with PBST, incubated with HRP conjugated donkey anti-goat (Jackson Immunoresearch) for 45 min at room temperature, followed by secondary antibody incubation. The slides were washed with TBST three times and incubated in DAB chromogen and peroxidase substrate (Santacruz Biotechnology) for 10-15 min. The slides were the washed in DI water 2-3 times and counterstained with Hematoxylin for 30 secs – 1 min. Finally, the slides were washed in DI water, dehydrated with ethanol and xylene and mounted with Prolong. Fluorescent and bright field images were obtained with a Nikon Plan-Apochromat 40X objective on Nikon Eclipse TE2000 widefield microscope equipped with a Hamamatsu C9000-02 EM-CCD camera. Bright field imaging to visualize DAB staining was performed using spot imaging software. To quantify protein expression, images were color deconvolved using the H DAB function in Fiji Image J software. The Optical density (OD) of the DAB channel was then measured on a per image basis.

2.10. Flow Cytometry

Cells were detached from the glass surface using warm Versene-EDTA (Lonza) for 5 min followed by fixation with 4 % paraformaldehyde for 10 min at 4° C. Cells were washed multiple times and resuspended in FACS buffer (Dulbecco's Phosphate Buffered Saline -Ca2+-Mg2+ supplemented with 1 % FBS and 5 mM EDTA). IVT mRNA labeled with Dylight-650 was used for flow cytometry experiments. Experiments were performed using a BD FACS-Canto II flow cytometer and the data were analyzed using the FlowJo software.

2.11. Synthesis of PA Hydrogel formulation functionalized with fibronectin or collagen

Cover glass (25 mm or 12 mm) were cleaned with plasma cleaner for 2.5 min and the glass surface was treated with APTES (VWR) for 5 min. The glass coverslips were washed in DI water 2-3 times, soaked in glutaraldehyde (Electron microcopy Solution, EMS) for 30 min at RT in a fume hood, washed once with DI water, dried and stored in a dessicator until used. PA hydrogels (1, 10 and 100 kPa) were prepared by mixing 40 % acrylamide and 2 % bis –acrylamide solution (Biorad) followed by addition of APS and TEMED (VWR) for gel polymerization [65,66]. A droplet of gel was placed on a cover glass which was flipped over a glass slide to form a gel "sandwich". Gels were polymerized for 30 min, washed with PBS 2-3 times and stored at 4^{o} C in PBS no longer than 7 days. On the day of cell seeding, gels were washed with 50mM HEPES (pH-8.5) for 2-3 times and incubated with 0.2 mg/ml Sulfo-SANPAH (Fisher Scientific). After Sulfo-SANPAH treatment, gels were immediately placed under 365 nm UV light source at a distance of approximately 3 inches and exposed for 10 min. Gels were washed with HEPES for 2-3 times and incubated with 20 µg/ml of fibronectin for minimum 3 h at 37^{o} C. Gels were finally washed with PBS twice and used as a substrate for cell plating.

2.12. RNA Sequencing of skeletal muscle cells on glass and Hydrogels

Total RNA was extracted from HskMSc cells grown either on 25 mm coverglass or on hydrogels using Qaigen RNAeasy kit. RNA concentration was measured using a nanodrop and the quality was tested on a Bioanalyser. 100 -200 ng of RNA resuspended in nuclease free water was used for sequencing. Samples were analyzed at the Integrated Genomic Core facility at the Yerkes Center at Emory University. RNAseq results obtained in Fastq format were converted to BAM files using the Galaxy software. The BAM files were run through the Cuffdiff software for differential transgene expression. The volcano plot for all genes was obtained, indicating the significantly expressed genes in cells plated on glass versus hydrogels. The final data were sorted for most significant differences in gene expression and run through Gene Set Enrichment Analysis (GSEA) which is a robust technique for analyzing gene expression data [67]. The software calculated an enrichment score (*ES*) reflecting the degree to which a set of genes is overrepresented at the extremes (top or bottom) of the entire ranked list *L*. The score is calculated by walking down the list *L* and the magnitude of the increment depends on the correlation of the gene with the phenotype. Multiple hypothesis testing was done by the software which yields normalized enrichment score (NES) controlling the proportion of false positives by calculating the false discovery rate (FDR). The FDR is the estimated probability that a set with a given *NES* represents a false positive finding.

2.13. Fluorescence in situ hybridization (FISH)

A549 cells (ATCC) were cultured in DMEM (Lonza) supplemented with 10 % FBS (Hyclone), 100 U/mL penicillin, and 100 µg/ml streptomycin (Life Technologies) and were plated on glass coverslips one day prior to transfection. Cells were transfected with 200 ng Dylight 650 pre-labeled IVT mRNA using Viromer RED (Lypocalyx), following the manufacturer protocol. Cells were fixed 6h post transfection using 70 % ethanol over-night at 4^{o} C. FISH was performed using 5 nM Quazar 570 Stellaris RNA probes (Biosearch Technology) complementary to the transcript coding region following the manufacturer protocol. Hybridization was performed overnight at 37^{o} C in a humid chamber. Female BALB/C mice were injected in the anterior tibialis, intramuscularly using 10 µg of cy3b labeled IVT mRNA complexed with Viromer RED in 40 µl of RiLa. The anterior tibialis muscle was removed 2 h post-delivery. Tissue was fixed in 4 % PFA overnight, followed by 30 % sucrose incubation overnight. Tissue was OTC embedded, snap frozen in dry ice chilled isopentane and stored at -80^{o} C. Sections 10 um in thickness were used for FISH following the manufacturer protocol. Tissue sections were permeabilized in 50 % methanol: 50 % acetone for 10 min at -20^{o} C. Hybridization was performed using 20 nM Quazar 670 Stellaris RNA probes complementary to the transcript coding region overnight at 37^{o} C in a humid chamber. Samples were stained with DAPI and mounted using Prolong gold. Samples were imaged as previously described.

2.14. Statistical Analysis

The data for luciferase assay, quantification of colocalization and quantification of the percentage of free /trapped mRNA were analyzed with Microsoft Excel and Sigmaplot. The statistically significant differences were tested with one-way and two-way ANOVA at p=0.05 followed by Holm-Sidak method for multiple comparison testing. All the luciferase assay experiments were performed three times in triplicates. Immunoflourescence experiments *in vitro* were performed three times in duplicates. Each animal experiment was performed on four mice. In RNAseq experiments, the nominal p value of the ES was calculated by the GSEA software by using an empirical phenotype-based permutation test procedure that preserves the complex correlation structure of the gene expression. The permutation of class labels provides a more biologically

reasonable assessment of significance than would be obtained when an entire database of gene sets is evaluated [67].

3. Results

3.1. Synthesis of CholK and DosK

To prepare CholK, the primary amine on the 6' position of Kanamycin A Sulfate 1 was selectively protected by a carboxybenzoyl (Cbz) group using *N*-benzyloxycarbonyloxy-5-norbornene-2,3-dicarboximide. The three remaining amino groups were then treated with 4-nitrophenyl 2-(trimethylsilyl)ethyl carbonate to yield a fully protected compound #3. Then, the Cbz group was removed by a classical hydrogenation reaction on supported Pd/C, giving the free aminomethyl derivative #4. The coupling of cholesteryl chloroformate with compound #4 led to the formation of the conjugate #5. Finally, CholK was obtained by deprotection of the Teoc groups using trifluoroacetic acid.

To prepare DosK reported in [21] the same procedure was followed as that of CholK except that the coupling of compound #4 with Cholesteryl Chloroformate was replaced by N-Succinyl-dioleylamine according to procedure extensively described in [27,28,63].

3.2. IVT mRNA expression in vivo and in vitro.

The firefly luciferase encoding IVT mRNA was labelled with three MTRIPs complementary to three sequences within the 3' UTR in order to visualize its distribution in cells in culture and mouse muscle. Cells and tissue were fixed 6h and 2h post-delivery, respectively. To verify that MTRIPs remain bound to mRNA upon delivery (modified PEI was used for the *in vitro* experiments, and IM injection *in vivo*), samples were subsequently hybridized over-night, post-fixation, with Stellaris RNA FISH probes specific for the coding region. MTRIPs colocalized extensively with the FISH probes signal (Fig. S1), while no fluorescence was observed in mock transfected cells. To further characterize the nanoparticles, the Zeta potential and mean particle size were measured. The Zeta potential of the mRNA complexed with CholK was -15.333 and complexed with DosK was 41.0333. The mean particle size of the mRNA plus CholK was 324 nm and mRNA plus DosK was 943 nm.

The labeled IVT mRNA either naked or complexed with nanocarriers was then used to study the protein expression *in vitro* and *in vivo*. *In vitro*, when delivered to HSkMSC cells, mRNA complexed with DosK led to efficient mRNA expression, while no protein production was observed with naked mRNA or mRNA complexed with CholK (Fig. 1A and B) at the single cell level by immunostaining (Fig. 1A) and via luciferase assay (Fig. 1B). Similar results were obtained in luciferase assays performed in myotubes (Fig. S8C) and Sol8 cells (Fig. S9C) delivered with mRNA naked, or complexed with nanoparticles. On the contrary, when injected intramuscularly in mice, naked mRNA or complexed with CholK yielded efficient luciferase expression by immunohistochemical staining, while no protein expression was detected with mRNA complexed with DosK (Fig. 1C and D). Interestingly, mRNA labeled with MTRIPs was clearly visible in tissues obtained from mice injected with naked mRNA or complexed with CholK, but not with DosK, indicating that nanocarriers affect mRNA entry, delivery and translatability in different fashions *in vivo* and *in vitro*. mRNA labelling with MTRIPs did not affect luciferase protein expression in HeLa cells (Fig. S2). The discrepancy between the observed efficiency of mRNA delivery and expression *in vivo* and *in vitro,* readily observable in our results, is a major concern for mRNA vaccine development.

3.3. Endosomal entry pathway differs in vitro and in vivo.

To further investigate the discrepancy between the results obtained *in vivo* and *in vitro*, the mRNA entry pathway was characterized upon delivery to HSkMSC cells and in mouse tissue, upon i.m. injection. IVT mRNA was fluorescently labeled with MTRIPs to observe its localization with respect to different endosomal components, such as clathrin (clathrin-light chain) and caveolin. I*n vitro,* mRNA delivered alone or complexed with DosK and CholK colocalized prevalently with caveolin, indicating that mRNA enters HSkMSC cells via a caveolin-mediated pathway (Fig. 2A). Similar results were observed for entry pathway in differentiated skeletal muscle cells, myotubes (Fig. S8A) and mouse muscle cell line, Sol8 (Fig. S9A). *In vivo*, mRNA delivered alone or complexed with CholK colocalized with clathrin, while mRNA complexed with DosK was mainly found outside the muscle tissue. Rare mRNA molecules delivered with DosK could be found within tissues but they did not colocalize with either clathrin or caveolin (Fig. 2B). The Mander's overlap coefficient used to quantify the colocalization between mRNA and different endosomal markers, confirmed our observations (Fig. 2C-D, Fig. S8B and S9B).

3.4. IVT mRNA release from endosomes in vitro and in vivo.

Caveolin and clathrin mediated endocytosis leads to exogenous mRNA trafficking to late endosomes and either degradation in the lysosomes or release in the cytosol. The fraction of mRNA trapped in endosomes or released can be determined by quantifying the colocalization of fluorescently labeled mRNA with early to mid-endosomal markers EEA1 and Rab5, and the late endosomal markers CD63 and Rab7 [68,69], upon immunostaining.

In HSkMSC cells, IVT mRNA delivered alone or complexed with CholK colocalized with endosomal markers at 6 h, indicating that it remained trapped in the endosomal compartment. IVT mRNA complexed with DosK were mostly free in the cell cytoplasm, demonstrating cytosolic release. The quantification of the percentage of free and trapped mRNA, confirmed that free mRNA was significantly higher *in vitro* for IVT mRNA complexed with DosK and lower for mRNA alone or complexed with CholK. On the contrary, *in vivo,* the percentage of free mRNA was significantly higher when mRNA was injected alone or complexed with CholK (Fig. 3A and B). Representative images of the experiments are shown in Fig. S3. Overall, the efficiency of mRNA release correlated with the efficiency of luciferase expression shown in Fig. 1, both *in vivo* and *in vitro*. Mander's overlap coefficient obtained from the colocalization analysis of mRNA and late endosomal markers both *in vitro* and *in vivo* showed similar trend for endosomal trapped mRNA (Fig. 3C).

To further characterize mRNA release from endosomal vesicles, we repeated the experiment in HSkMSC cells and performed immunostaining 1.5 h hours post-delivery. IVT mRNAs alone, complexed with DosK or CholK colocalized with all endosomal markers, indicating that, at this early time point, all mRNA is mainly trapped in endosomal vesicles (Fig. S4), independent of the delivery vehicle. Similar results were obtained *in vivo*, when mRNA alone or complexed with CholK was injected i.m. As previously observed, mRNA complexed with DosK was instead observed outside the muscle tissue (Fig. S5).

3.5. Effect of ECM proteins on endosomal entry pathway, release and protein production

The data shown so far clearly highlight differences in the mechanisms of IVT mRNA endocytosis/trafficking *in vitro* and *in vivo*, dependent on the delivery vehicle, and, as a consequence, differences in protein expression efficiency. The extracellular matrix proteins play an important role in enhanced protein production of transfected plasmid [42]. We hypothesized that the observed protein production *in vivo* could be due to presence of abundant ECM proteins in muscle tissue. Therefore, HSkMSC cells were plated on fibronectin or collagen, to determine if this would affect the IVT mRNA endosomal entry pathway, causing enhanced mRNA release in the cell cytosol and boost in protein production.

Fluorescently labeled IVT mRNA transfected alone, complexed with CholK and DosK were delivered to HSkMC cells and immunostaining for the endosomal components was performed as previously described. Colocalization analysis revealed a switch in the entry pathway from caveolin to clathrin-coated vesicles (Fig. S6) and endosomal release (Fig. S7). This observation was supported by the quantification of the Mander's overlap coefficient (Fig. 4A).

The quantification of the percentage of free and endosome-trapped mRNA revealed that, despite switching the entry pathway, both naked mRNA and complexed with CholK were not efficiently released in the cell cytoplasm 6h post-delivery. Interestingly, mRNA complexed with DosK was released more efficiently in the cytoplasm of cells plated on fibronectin than on collagen (Fig. 4B and C). As expected, mRNA transfected alone or with CholK were not expressed efficiently (Fig. 4D), as previously observed using cells plated on an uncoated surface (Fig. 1A). Interestingly, mRNA complexed with DosK was expressed more efficiently in cells plated on uncoated or fibronectin-coated surfaces, but yielded significantly lower protein expression in cells plated on collagen-coated surfaces (Fig. 4D). In summary, these results indicate that the presence of fibronectin induced a switch of the entry mechanism from caveolin to clathrin-mediated pathway but, overall, did not alter the expression efficiency of the delivered mRNA *in vitro*, suggesting that the presence of ECM proteins is not sufficient to mimic the *in vivo* microenvironment.

3.6. Protein expression, IVT mRNA endosomal entry and release of muscle cells on Hydrogels

Next, we investigated how the extracellular matrix stiffness influences mRNA entry/trafficking/release and, as a consequence, protein synthesis. PA hydrogels functionalized with 20 µg/ml fibronectin and with a stiffness of 10 kPa were utilized as substrate to grow HSkMSC muscle cells [65], with the hypothesis that this would mimic the results obtained in our *in vivo* model. mRNA entry pathway, mRNA release and protein production on hydrogels were studied and compared to the results obtained using cells plated on an untreated glass surface. Skeletal muscle cells were cultured on hydrogels of varying stiffness (1, 10 and 100 kPa) and glass (> 10 GPa) and were transfected with IVT mRNA complexed with CholK. Luciferase expression, measured at 24 h, was significantly higher in cells cultured on 10 kPa hydrogels compared to 1 and 100 kPa (Fig. S10); this result confirms that mRNA translation depends on the stiffness of the substrate and that 10 kPa was the optimal stiffness for culturing HSkMSC cells for subsequent experiments.

The luciferase reporter activity measured 24h post-delivery in cells transfected with IVT mRNA alone or with CholK plated on hydrogels was significantly higher than that observed for cells plated on glass, while it decreased using mRNA complexed with DosK (Fig. 5A). Immunostaining for the endosomal entry markers caveolin and clathrin (Fig. 5C) and quantification of the colocalization between fluorescently labeled mRNA and caveolin or clathrin by Mander's overlap coefficient (Fig. 5E) revealed that mRNA uptake was prevalently clathrin-mediated.

This was confirmed by treating cells plated on hydrogels with drugs that selectively inhibit either clathrin or caveolin-mediated vesicle formation. As expected, mRNA expression decreased significantly in cells preincubated in media containing the clathrin inhibitor "chlorpromazine", while remained unchanged in cells preincubated in media containing the caveolin inhibitor "genestein" (Fig. 5B).

We quantified mRNA release from the endosomal system 6h post-delivery by immunostaining with mid to late endosomal markers in cells plated on hydrogels. The results showed that mRNA delivered alone or with CholK were readily released in the cell cytosol, whereas less endosomal release was observed with DosK (Fig. 5D and F). Thus, when mRNA was delivered naked or complexed with CholK, protein expression was efficient. Interestingly, when mRNA was delivered with Dosk, the luciferase activity was not completely abrogated, as observed *in vivo*, but it was significantly reduced.

3.7. Factors associated with efficient translation of IVT mRNA on softer substrate Hydrogels

Next, HSkMSC muscle cells on glass or hydrogel were transfected with labeled IVT mRNA either naked or complexed with CholK and mRNA uptake was measured using flow cytometry. mRNA uptake occurred more efficiently in cells plated on hydrogels (10 kPa stiffness) than on untreated glass coverslip (Fig. 6A) minimizing the differences between *in vitro* and *in vivo* results [53]. Cytoskeletal integrity, gene regulation and cell morphology are deeply influenced by substrate stiffness [70]. Since some transcriptional cofactors and ECM related genes are upregulated on softer substrates [71], RNAseq was performed on cells plated on hydrogels or on glass coverslips to identify which genes were upregulated. GSEA analysis showed a significant

overexpression of genes involved in Kegg ribosome, translation, metabolism of translation and 3' UTR-mediated translational regulation pathways with p value of 0 (Table 3).

The main genes enriched in the translational pathways are listed in Table 4. The data is also represented as a volcano plot indicating the significantly overexpressed genes in cells plated on hydrogels compared to glass coverslips (Fig. 6B). Interestingly, significant upregulation was found for several translational initiation factors including EIF2S3, EIF4H, EIF4A1, EIF3Dand EIF4G1, endosomal clathrin (CLTA), the ECM protein collagen (COL1A1, COL1A2) and ribosomal genes including RPL26, RPL27, RPL29, and RPS3A.

4. Discussion

Characterizing the formulation of IVT mRNA complexed with nanocarriers *in vitro* is vital for the development of mRNA-based vaccines, but such screening has limitations due to the differences in protein expression observed *in vitro* (plated on glass or plastic) and i*n vivo.* The data described in Table 1 clearly indicate that results of experiments *in vitro* frequently cannot be used to infer or predict the outcome of experiments *in vivo*, independently on the nanocarrier utilized for the delivery. The results presented here, obtained using both naked IVT mRNA and complexed with two delivery vehicles, CholK and DosK are summarized in Table 5, are consistent with this conclusion.

The endocytic pathway and subsequent release into the cytosol are closely related to mRNA intracellular fate and, therefore, to protein expression [72,73]. We observed that clathrin-mediated endocytosis led to high protein expression, *in vivo*, while caveolin-mediated endocytosis resulted in poor protein expression *in vitro,* for IVT mRNA delivered with CholK. On the contrary, IVT mRNA delivered with DosK entered through the caveolin pathway and expressed efficiently *in vitro,* but failed in vivo, highlighting the differences in endocytic pathway and protein expression *in vitro* and *in vivo* (Fig. 1 and 2). We demonstrated that the IVT mRNA complexed with DosK did not penetrate tissues efficiently (Fig.2B and D). These results were not surprising as we observed consistently that protein synthesis correlated positively with the amount of mRNA present in the cell cytoplasm and released in time from the endocytic system (Fig. 1 and 3).

Interestingly, culturing cells on either fibronectin or collagen, two essential components of the ECM abundant in muscle tissue, was sufficient to cause a switch in the entry pathway from caveolin to clathrin (Fig. 4), but not to induce a boost in mRNA release and subsequent protein production, nor to obtain results that recapitulate those obtained *in vivo*. This implied that the entry mechanism alone was not sufficient to explain the differences in protein expression observed *in vivo*. Moreover, the addition of ECM proteins to cultured cells was not sufficient to overcome the limits of this *in vitro* model system.

Indeed, one of the main limits of experiments performed *in vitro* using cell lines, is the substrate on which cells are cultured (typically glass or plastic), which frequently prohibits the cells from exhibiting the physiological properties of functional tissues *in vivo*. This limitation can be alleviated by the design of biomaterials which could recapitulate *in vivo* mechanobiological properties. For an initial, high-through-put screening of nanocarriers *in vitro* toward the development of vaccine formulations, simple and affordable biomaterials exhibiting physiochemical and mechanical properties closely resembling *in vivo* tissue can be utilized.

Hydrogels have been used for culturing skeletal muscle, myoblast and myotubes. For example, it's been shown that myotubes plated on stiff substrates differentiate into myotubes with very few striations, whereas a typical sarcomere banding pattern was observed for myotubes cultured on softer substrates [74]. Tissue compliance has also been shown to play an important role in DNA uptake and expression. Multiple studies have shown that plasmids transfected into cells plated on a soft substrate express protein more efficiently than on a stiffer substrate [53,54,55]. Studies reported earlier showed that hydrogels of Elastic modulus of 10 kPa

for myoblast and 12 kPa for myotubes strengthen adhesion, cell spreading and traction force which recapitulate the mechanosensitive property of muscle tissue [75,76].

Among the various natural or synthetic materials that can be used to assemble hydrogels, polyacrylamide (PA) allows for a simple fabrication procedure with well- established protocols to produce statistically compliant 2D substrates with tunable stiffness. While 3D hydrogels may more accurately model the architecture of some tissues and present milieus that lead to more realistic cellular responses, here, 2D hydrogels permitted straightforward harvesting of cultured cells for luciferase assays or other downstream procedures. Moreover, they represent suitable substrates for high resolution confocal microscopy analysis, which could be performed with no alterations of the immunofluorescence protocols to compare the results obtained *in vitro* and *in vivo*.

Consistent with the cited studies, we found that IVT mRNA delivered into muscle cells plated on hydrogels of 10 kPa yielded efficient protein production (Fig. 5A), with an overall trend similar to the one observed *in vivo*. Further studies using endosomal entry markers suggested that mRNA entered predominantly via a clathrin mediated pathway, and was released efficiently, as soon as 6 h post-delivery (Fig. 5 E-F). Interestingly, clathrin and not caveolin mediated endocytosis yielded efficient protein production in this model system, as observed in the results obtained *in vivo*. However, as expected, mRNA uptake per cell on hydrogels was more efficient than on glass, which could explain the enhanced protein production obtained on hydrogel (Fig. 6A).

Overall, our results confirm that the composition and stiffness of the substrate on which cells are cultured plays a critical role to characterize various formulations of IVT mRNA complexed with nanocarriers *in vitro,* to successfully predict mRNA expression *in vivo*. Cellular uptake and expression of nanocomplexes depend on their physiochemical properties as well as on the biomechanical properties of cell membranes, including cell membrane surface area, membrane tension, bending modulus [77,78], focal adhesion [45,47,52] and elasticity [51,59]. All these properties can be modulated by varying the stiffness of the substrate. According to our findings, the difference in stiffness of glass and the hydrogels may explain the differences between the results obtained *in vitro* and *in vivo*, indicating that hydrogels may represent a suitable tool for the initial characterization, *in vitro,* of various IVT mRNA/delivery vehicle complexes. Mechanotransduction is known to affects various cellular processes like motility, adhesion, proliferation, migration, apoptosis, and differentiation [45,46,47,48] and to influence the efficiency of plasmid expression [54,55,79]. However, little is known about the effects on the regulation of translational mechanisms upon IVT mRNA delivery. The results obtained by RNAseq suggest that cells cultured on hydrogel significantly overexpressed genes involved in mRNA translation, compared to those cultured on glass, indicating that mechanical forces applied to cells influence the activation of mRNA translational pathways. The analysis of data on GSEA confirmed a strong positive correlation between enhanced RNA translation pathway and expression of ribosomal genes (Fig. 6B).

5. Conclusion

Our results demonstrate that IVT mRNA uptake, trafficking, endosomal release and expression *in vitro* using a hydrogel model leads to expression of both naked mRNA or mRNA complexed with CholK and a significant decrease in protein production with mRNA complexed to DosK, as observed *in vivo*. We conclude that the differences observed *in vitro* and *in vivo* depend on tissue stiffness, which initiates mechanosensitive signals resulting in improved uptake of IVT mRNA and upregulation of translation related genes. Thus, these study highlights some of the factors responsible for *in vivo* and *in vitr*o discrepancies and, will assist in the characterization of IVT mRNA based vaccines *in vitro* using tunable hydrogel models.

Funding: This work was supported by Defense Advanced Research Projects Agency (DARPA), Sanofi Pasteur, and the RNArmorVax Consortium. This material is based upon work supported by the National Science Foundation Graduate Research Fellowship Program under Grant No. DGE-1650044. The views, opinions, and/or findings expressed are those of the author(s) and should not be interpreted as representing

the official views or policies of the Department of Defense, the National Science Foundation and the U.S. Government.

Conflict of Interest: D.H. and B.P. are employees of In-Cell-Art, which commercializes lipidic aminoglycoside derivatives. P.B. is an employee of CureVac, which commercializes RNA-based vaccines. D.E. is an employee of Sanofi Pasteur, which commercializes vaccines.

Contributors

S.M.B., P.J.S. and B.P. conceived the project, designed experiments, and wrote the manuscript. K.H.L. assisted with mice experiments. J.L.K. contributed for the flow experiment and E.L.B. assisted in FISH experiment. D.A.V. contributed for statistical analysis and C.Z. assisted with critical editing of the manuscript. D.H. and P.B. produced the delivery vehicles and mRNA, respectively. D.E. assisted with all protocols for using nanomaterial. All other experiments were performed by S.M.B in consultation with P.J.S. All authors have approved the final article.

References

[1] I. Hoerr, R. Obst, H.G. Rammensee, G. Jung, *In vivo* application of RNA leads to induction of specific cytotoxic T lymphocytes and antibodies, Eur J Immunol 30 (2000) 1-7.

[2] B. Petsch, M. Schnee, A.B. Vogel, E. Lange, B. Hoffmann, D. Voss, T. Schlake, A. Thess, K.J. Kallen, L. Stitz, T. Kramps, Protective efficacy of *in vitro* synthesized, specific mRNA vaccines against influenza A virus infection, Nat Biotechnol 30 (2012) 1210-1216.

[3] K. Bahl, J.J. Senn, O. Yuzhakov, A. Bulychev, L.A. Brito, K.J. Hassett, M.E. Laska, M. Smith, O. Almarsson, J. Thompson, A.M. Ribeiro, M. Watson, T. Zaks, G. Ciaramella, Preclinical and Clinical Demonstration of Immunogenicity by mRNA Vaccines against H10N8 and H7N9 Influenza Viruses, Mol Ther (2017).

[4] X. Su, J. Fricke, D.G. Kavanagh, D.J. Irvine, *In vitro* and *in vivo* mRNA delivery using lipid-enveloped pH-responsive polymer nanoparticles, Mol Pharm 8 (2011) 774-787.

[5] L. Wasungu, D. Hoekstra, Cationic lipids, lipoplexes and intracellular delivery of genes, J Control Release 116 (2006) 255-264.

[6] S.E. Jin, C.K. Kim, Charge-mediated topical delivery of plasmid DNA with cationic lipid nanoparticles to the skin, Colloids Surf B Biointerfaces 116 (2014) 582-590.

[7] A. Fasbender, J. Zabner, B.G. Zeiher, M.J. Welsh, A low rate of cell proliferation and reduced DNA uptake limit cationic lipid-mediated gene transfer to primary cultures of ciliated human airway epithelia, Gene Ther 4 (1997) 1173-1180.

[8] D. Luo, W.M. Saltzman, Synthetic DNA delivery systems, Nat Biotechnol 18 (2000) 33-37.

[9] J.A. Wolff, R.W. Malone, P. Williams, W. Chong, G. Acsadi, A. Jani, P.L. Felgner, Direct gene transfer into mouse muscle *in vivo*, Science 247 (1990) 1465-1468.

[10] F.W. Johanning, R.M. Conry, A.F. LoBuglio, M. Wright, L.A. Sumerel, M.J. Pike, D.T. Curiel, A Sindbis virus mRNA polynucleotide vector achieves prolonged and high level heterologous gene expression *in vivo*, Nucleic Acids Res 23 (1995) 1495-1501.

[11] J.Y. Je, Y.S. Cho, S.K. Kim, Characterization of (aminoethyl)chitin/DNA nanoparticle for gene delivery, Biomacromolecules 7 (2006) 3448-3451.

[12] Tarwadi, J.A. Jazayeri, R.J. Prankerd, C.W. Pouton, Preparation and *in vitro* evaluation of novel lipopeptide transfection agents for efficient gene delivery, Bioconjug Chem 19 (2008) 940-950.

[13] G. Shim, H.W. Choi, S. Lee, J. Choi, Y.H. Yu, D.E. Park, Y. Choi, C.W. Kim, Y.K. Oh, Enhanced intrapulmonary delivery of anticancer siRNA for lung cancer therapy using cationic ethylphosphocholine-based nanolipoplexes, Mol Ther 21 (2013) 816-824.

[14] B. Schwartz, C. Benoist, B. Abdallah, D. Scherman, J.P. Behr, B.A. Demeneix, Lipospermine-based gene transfer into the newborn mouse brain is optimized by a low lipospermine/DNA charge ratio, Hum Gene Ther 6 (1995) 1515-1524.

[15] Y. Hattori, W.X. Ding, Y. Maitani, Highly efficient cationic hydroxyethylated cholesterol-based nanoparticle-mediated gene transfer *in vivo* and *in vitro* in prostate carcinoma PC-3 cells, J Control Release 120 (2007) 122-130.
[16] L. Wightman, R. Kircheis, V. Rossler, S. Carotta, R. Ruzicka, M. Kursa, E. Wagner, Different behavior of branched and linear polyethylenimine for gene delivery *in vitro* and *in vivo*, J Gene Med 3 (2001) 362-372.
[17] T. Gjetting, N.S. Arildsen, C.L. Christensen, T.T. Poulsen, J.A. Roth, V.N. Handlos, H.S. Poulsen, *In vitro* and *in vivo* effects of polyethylene glycol (PEG)-modified lipid in DOTAP/cholesterol-mediated gene transfection, Int J Nanomedicine 5 (2010) 371-383.
[18] B. Pitard, H. Pollard, O. Agbulut, O. Lambert, J.T. Vilquin, Y. Cherel, J. Abadie, J.L. Samuel, J.L. Rigaud, S. Menoret, I. Anegon, D. Escande, A nonionic amphiphile agent promotes gene delivery *in vivo* to skeletal and cardiac muscles, Hum Gene Ther 13 (2002) 1767-1775.
[19] C. Lorenz, M. Fotin-Mleczek, G. Roth, C. Becker, T.C. Dam, W.P. Verdurmen, R. Brock, J. Probst, T. Schlake, Protein expression from exogenous mRNA: uptake by receptor-mediated endocytosis and trafficking via the lysosomal pathway, RNA Biol 8 (2011) 627-636.
[20] E. Frohlich, The role of surface charge in cellular uptake and cytotoxicity of medical nanoparticles, Int J Nanomedicine 7 (2012) 5577-5591.
[21] R.G. Parton, K. Simons, The multiple faces of caveolae, Nat Rev Mol Cell Biol 8 (2007) 185-194.
[22] J. Rejman, A. Bragonzi, M. Conese, Role of clathrin- and caveolae-mediated endocytosis in gene transfer mediated by lipo- and polyplexes, Mol Ther 12 (2005) 468-474.
[23] L. Billiet, J.P. Gomez, M. Berchel, P.A. Jaffres, T. Le Gall, T. Montier, E. Bertrand, H. Cheradame, P. Guegan, M. Mevel, B. Pitard, T. Benvegnu, P. Lehn, C. Pichon, P. Midoux, Gene transfer by chemical vectors, and endocytosis routes of polyplexes, lipoplexes and lipopolyplexes in a myoblast cell line, Biomaterials 33 (2012) 2980-2990.
[24] G. Pilcer, R. Rosiere, K. Traina, T. Sebti, F. Vanderbist, K. Amighi, New co-spray-dried tobramycin nanoparticles-clarithromycin inhaled powder systems for lung infection therapy in cystic fibrosis patients, J Pharm Sci 102 (2013) 1836-1846.
[25] J.N. Payne, H.K. Waghwani, M.G. Connor, W. Hamilton, S. Tockstein, H. Moolani, F. Chavda, V. Badwaik, M.B. Lawrenz, R. Dakshinamurthy, Novel Synthesis of Kanamycin Conjugated Gold Nanoparticles with Potent Antibacterial Activity, Front Microbiol 7 (2016) 607.
[26] L. Desigaux, M. Sainlos, O. Lambert, R. Chevre, E. Letrou-Bonneval, J.P. Vigneron, P. Lehn, J.M. Lehn, B. Pitard, Self-assembled lamellar complexes of siRNA with lipidic aminoglycoside derivatives promote efficient siRNA delivery and interference, Proc Natl Acad Sci U S A 104 (2007) 16534-16539.
[27] D. Habrant, P. Peuziat, T. Colombani, L. Dallet, J. Gehin, E. Goudeau, B. Evrard, O. Lambert, T. Haudebourg, B. Pitard, Design of Ionizable Lipids To Overcome the Limiting Step of Endosomal Escape: Application in the Intracellular Delivery of mRNA, DNA, and siRNA, J Med Chem 59 (2016) 3046-3062.
[28] M. Mevel, M. Sainlos, B. Chatin, N. Oudrhiri, M. Hauchecorne, O. Lambert, J.P. Vigneron, P. Lehn, B. Pitard, J.M. Lehn, Paromomycin and neomycin B derived cationic lipids: synthesis and transfection studies, J Control Release 158 (2012) 461-469.
[29] P.J. Santangelo, A.W. Lifland, P. Curt, Y. Sasaki, G.J. Bassell, M.E. Lindquist, J.E. Crowe, Jr., Single molecule-sensitive probes for imaging RNA in live cells, Nat Methods 6 (2009) 347-349.
[30] P.J. Santangelo, E. Alonas, J. Jung, A.W. Lifland, C. Zurla, Probes for intracellular RNA imaging in live cells, Methods Enzymol 505 (2012) 383-399.
[31] C. Zurla, A.W. Lifland, P.J. Santangelo, Characterizing mRNA interactions with RNA granules during translation initiation inhibition, PLoS One 6 (2011) e19727.
[32] A.W. Lifland, C. Zurla, J. Yu, P.J. Santangelo, Dynamics of native beta-actin mRNA transport in the cytoplasm, Traffic 12 (2011) 1000-1011.
[33] J. Jung, A.W. Lifland, C. Zurla, E.J. Alonas, P.J. Santangelo, Quantifying RNA-protein interactions in situ using modified-MTRIPs and proximity ligation, Nucleic Acids Res 41 (2013) e12.

[34] J. Jung, A.W. Lifland, E.J. Alonas, C. Zurla, P.J. Santangelo, Characterization of mRNA-cytoskeleton interactions in situ using FMTRIP and proximity ligation, PLoS One 8 (2013) e74598.
[35] C. Zurla, J. Jung, E.L. Blanchard, P.J. Santangelo, A Novel Method to Quantify RNA-Protein Interactions In Situ Using FMTRIP and Proximity Ligation, Methods Mol Biol 1468 (2017) 155-170.
[36] C. Zurla, J. Jung, P.J. Santangelo, Can we observe changes in mRNA "state"? Overview of methods to study mRNA interactions with regulatory proteins relevant in cancer related processes, Analyst 141 (2016) 548-562.
[37] A.W. Lifland, J. Jung, E. Alonas, C. Zurla, J.E. Crowe, Jr., P.J. Santangelo, Human respiratory syncytial virus nucleoprotein and inclusion bodies antagonize the innate immune response mediated by MDA5 and MAVS, J Virol 86 (2012) 8245-8258.
[38] E. Alonas, A.W. Lifland, M. Gudheti, D. Vanover, J. Jung, C. Zurla, J. Kirschman, V.F. Fiore, A. Douglas, T.H. Barker, H. Yi, E.R. Wright, J.E. Crowe, Jr., P.J. Santangelo, Combining single RNA sensitive probes with subdiffraction-limited and live-cell imaging enables the characterization of virus dynamics in cells, ACS Nano 8 (2014) 302-315.
[39] J.L. Kirschman, S. Bhosle, D. Vanover, E.L. Blanchard, K.H. Loomis, C. Zurla, K. Murray, B.C. Lam, P.J. Santangelo, Characterizing exogenous mRNA delivery, trafficking, cytoplasmic release and RNA-protein correlations at the level of single cells, Nucleic Acids Res (2017).
[40] A. Dhaliwal, M. Maldonado, Z. Han, T. Segura, Differential uptake of DNA-poly(ethylenimine) polyplexes in cells cultured on collagen and fibronectin surfaces, Acta Biomater 6 (2010) 3436-3447.
[41] E.H. Chowdhury, M. Nagaoka, K. Ogiwara, F.T. Zohra, K. Kutsuzawa, S. Tada, C. Kitamura, T. Akaike, Integrin-supported fast rate intracellular delivery of plasmid DNA by extracellular matrix protein embedded calcium phosphate complexes, Biochemistry 44 (2005) 12273-12278.
[42] F.T. Zohra, Y. Maitani, T. Akaike, mRNA delivery through fibronectin associated liposome-apatite particles: a new approach for enhanced mRNA transfection to mammalian cell, Biol Pharm Bull 35 (2012) 111-115.
[43] Z. Bengali, J.C. Rea, L.D. Shea, Gene expression and internalization following vector adsorption to immobilized proteins: dependence on protein identity and density, J Gene Med 9 (2007) 668-678.
[44] E. Uchimura, S. Yamada, L. Uebersax, T. Yoshikawa, K. Matsumoto, M. Kishi, D.P. Funeriu, M. Miyake, J. Miyake, On-chip transfection of PC12 cells based on the rational understanding of the role of ECM molecules: efficient, non-viral transfection of PC12 cells using collagen IV, Neurosci Lett 378 (2005) 40-43.
[45] H.J. Kong, T.R. Polte, E. Alsberg, D.J. Mooney, FRET measurements of cell-traction forces and nano-scale clustering of adhesion ligands varied by substrate stiffness, Proc Natl Acad Sci U S A 102 (2005) 4300-4305.
[46] D.E. Ingber, Mechanobiology and diseases of mechanotransduction, Ann Med 35 (2003) 564-577.
[47] M.A. Schwartz, Integrins and extracellular matrix in mechanotransduction, Cold Spring Harb Perspect Biol 2 (2010) a005066.
[48] S. Kumar, Cellular mechanotransduction: stiffness does matter, Nat Mater 13 (2014) 918-920.
[49] A. Mammoto, T. Mammoto, D.E. Ingber, Mechanosensitive mechanisms in transcriptional regulation, J Cell Sci 125 (2012) 3061-3073.
[50] Y.R. Shih, K.F. Tseng, H.Y. Lai, C.H. Lin, O.K. Lee, Matrix stiffness regulation of integrin-mediated mechanotransduction during osteogenic differentiation of human mesenchymal stem cells, J Bone Miner Res 26 (2011) 730-738.
[51] H.J. Kong, J. Liu, K. Riddle, T. Matsumoto, K. Leach, D.J. Mooney, Non-viral gene delivery regulated by stiffness of cell adhesion substrates, Nat Mater 4 (2005) 460-464.
[52] K.R. Levental, H. Yu, L. Kass, J.N. Lakins, M. Egeblad, J.T. Erler, S.F. Fong, K. Csiszar, A. Giaccia, W. Weninger, M. Yamauchi, D.L. Gasser, V.M. Weaver, Matrix crosslinking forces tumor progression by enhancing integrin signaling, Cell 139 (2009) 891-906.
[53] J.L. Brugnano, A. Panitch, Matrix stiffness affects endocytic uptake of MK2-inhibitor peptides, PLoS One 9 (2014) e84821.

[54] J. Zhang, A. Sen, E. Cho, J.S. Lee, K. Webb, Poloxamine/fibrin hybrid hydrogels for non-viral gene delivery, J Tissue Eng Regen Med (2014).
[55] C. Chu, H. Kong, Interplay of cell adhesion matrix stiffness and cell type for non-viral gene delivery, Acta Biomater 8 (2012) 2612-2619.
[56] S. Musah, S.A. Morin, P.J. Wrighton, D.B. Zwick, S. Jin, L.L. Kiessling, Glycosaminoglycan-binding hydrogels enable mechanical control of human pluripotent stem cell self-renewal, ACS Nano 6 (2012) 10168-10177.
[57] R. Gauvin, R. Parenteau-Bareil, M.R. Dokmeci, W.D. Merryman, A. Khademhosseini, Hydrogels and microtechnologies for engineering the cellular microenvironment, Wiley Interdiscip Rev Nanomed Nanobiotechnol 4 (2012) 235-246.
[58] A.M. Cozzolino, V. Noce, C. Battistelli, A. Marchetti, G. Grassi, C. Cicchini, M. Tripodi, L. Amicone, Modulating the Substrate Stiffness to Manipulate Differentiation of Resident Liver Stem Cells and to Improve the Differentiation State of Hepatocytes, Stem Cells Int 2016 (2016) 5481493.
[59] A. Buxboim, I.L. Ivanovska, D.E. Discher, Matrix elasticity, cytoskeletal forces and physics of the nucleus: how deeply do cells 'feel' outside and in?, J Cell Sci 123 (2010) 297-308.
[60] A.J. Engler, S. Sen, H.L. Sweeney, D.E. Discher, Matrix elasticity directs stem cell lineage specification, Cell 126 (2006) 677-689.
[61] K. Kariko, H. Muramatsu, J. Ludwig, D. Weissman, Generating the optimal mRNA for therapy: HPLC purification eliminates immune activation and improves translation of nucleoside-modified, protein-encoding mRNA, Nucleic Acids Res 39 (2011) e142.
[62] M. Sainlos, P. Belmont, J.-P. Vigneron, P. Lehn, J.-M. Lehn, Aminoglycoside-Derived Cationic Lipids for Gene Transfection: Synthesis of Kanamycin A Derivatives, European Journal of Organic Chemistry 2003 (2003) 2764-2774.
[63] T. Colombani, P. Peuziat, L. Dallet, T. Haudebourg, M. Mevel, M. Berchel, O. Lambert, D. Habrant, B. Pitard, Self-assembling complexes between binary mixtures of lipids with different linkers and nucleic acids promote universal mRNA, DNA and siRNA delivery, J Control Release 249 (2017) 131-142.
[64] V.K. Udhayakumar, A. De Beuckelaer, J. McCaffrey, C.M. McCrudden, J.L. Kirschman, D. Vanover, L. Van Hoecke, K. Roose, K. Deswarte, B.G. De Geest, S. Lienenklaus, P.J. Santangelo, J. Grooten, H.O. McCarthy, S. De Koker, Arginine-Rich Peptide-Based mRNA Nanocomplexes Efficiently Instigate Cytotoxic T Cell Immunity Dependent on the Amphipathic Organization of the Peptide, Adv Healthc Mater (2017).
[65] J.R. Tse, A.J. Engler, Preparation of hydrogel substrates with tunable mechanical properties, Curr Protoc Cell Biol Chapter 10 (2010) Unit 10 16.
[66] C.E. Kandow, P.C. Georges, P.A. Janmey, K.A. Beningo, Polyacrylamide hydrogels for cell mechanics: steps toward optimization and alternative uses, Methods Cell Biol 83 (2007) 29-46.
[67] A. Subramanian, P. Tamayo, V.K. Mootha, S. Mukherjee, B.L. Ebert, M.A. Gillette, A. Paulovich, S.L. Pomeroy, T.R. Golub, E.S. Lander, J.P. Mesirov, Gene set enrichment analysis: a knowledge-based approach for interpreting genome-wide expression profiles, Proc Natl Acad Sci U S A 102 (2005) 15545-15550.
[68] S. Das, P.E. Pellett, Spatial relationships between markers for secretory and endosomal machinery in human cytomegalovirus-infected cells versus those in uninfected cells, J Virol 85 (2011) 5864-5879.
[69] A. Macovei, C. Petrareanu, C. Lazar, P. Florian, N. Branza-Nichita, Regulation of hepatitis B virus infection by Rab5, Rab7, and the endolysosomal compartment, J Virol 87 (2013) 6415-6427.
[70] J.T. Davis, Q. Wen, P.A. Janmey, D.C. Otteson, W.J. Foster, Muller cell expression of genes implicated in proliferative vitreoretinopathy is influenced by substrate elastic modulus, Invest Ophthalmol Vis Sci 53 (2012) 3014-3019.
[71] V.K. Raghunathan, J.T. Morgan, B. Dreier, C.M. Reilly, S.M. Thomasy, J.A. Wood, I. Ly, B.C. Tuyen, M. Hughbanks, C.J. Murphy, P. Russell, Role of substratum stiffness in modulating genes associated with extracellular matrix and mechanotransducers YAP and TAZ, Invest Ophthalmol Vis Sci 54 (2013) 378-386.

[72] K.J. Kauffman, M.J. Webber, D.G. Anderson, Materials for non-viral intracellular delivery of messenger RNA therapeutics, J Control Release (2015).
[73] O. Harush-Frenkel, E. Rozentur, S. Benita, Y. Altschuler, Surface charge of nanoparticles determines their endocytic and transcytotic pathway in polarized MDCK cells, Biomacromolecules 9 (2008) 435-443.
[74] E. Serena, S. Zatti, E. Reghelin, A. Pasut, E. Cimetta, N. Elvassore, Soft substrates drive optimal differentiation of human healthy and dystrophic myotubes, Integr Biol (Camb) 2 (2010) 193-201.
[75] A.J. Engler, M.A. Griffin, S. Sen, C.G. Bonnemann, H.L. Sweeney, D.E. Discher, Myotubes differentiate optimally on substrates with tissue-like stiffness: pathological implications for soft or stiff microenvironments, J Cell Biol 166 (2004) 877-887.
[76] A. Engler, L. Bacakova, C. Newman, A. Hategan, M. Griffin, D. Discher, Substrate compliance versus ligand density in cell on gel responses, Biophys J 86 (2004) 617-628.
[77] S. Zhang, H. Gao, G. Bao, Physical Principles of Nanoparticle Cellular Endocytosis, ACS Nano 9 (2015) 8655-8671.
[78] C. Huang, P.J. Butler, S. Tong, H.S. Muddana, G. Bao, S. Zhang, Substrate stiffness regulates cellular uptake of nanoparticles, Nano Lett 13 (2013) 1611-1615.
[79] S. Gojgini, T. Tokatlian, T. Segura, Utilizing cell-matrix interactions to modulate gene transfer to stem cells inside hyaluronic acid hydrogels, Mol Pharm 8 (2011) 1582-1591.

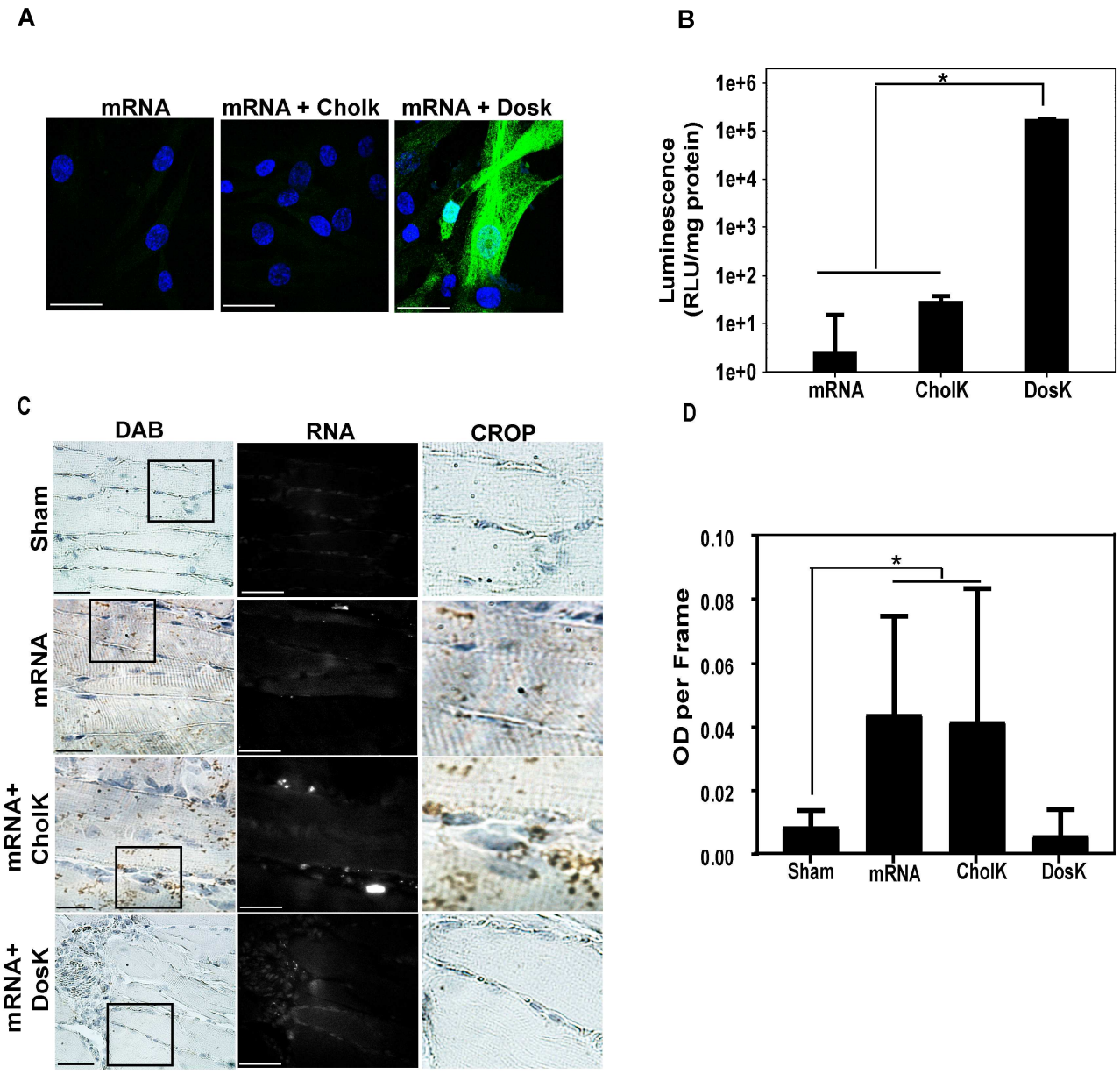

Fig. 1. IVT mRNA expression differs *in vitro* and *in vivo.* A) Luciferase mRNA (500 ng) was delivered to HSkMSC cells alone or complexed with CholK or DosK. Protein expression is shown in green and nuclei are stained with DAPI in blue. Scale bars are 15 µm**.** Experiment was performed three times in duplicate**.** B) The Luciferase activity was detected by bright glo luciferase assay system and the reads were normalized to untransfected controls.* Indicates $p < 0.05$, tested by one-way ANOVA followed by Holm-Sidak multiple comparison testing**.** Luciferase assay experiments were performed three times in triplicates. C) Mice were injected, i.m., with 10 µg dylight 680 labeled mRNA, naked or complexed with CholK or DosK. IHC was performed on muscle tissue extracted 16 h post-delivery. Tissue sections (3 to 4) from 4 mice per condition were used for IHC staining. Representative bright field images of DAB staining (brown) were obtained from the same section with spot software and mRNA (white) was imaged using the Volocity software. Scale bars are 20 µm. D) Images (3-4) per condition were quantified with Fiji Image J software and average OD plotted.

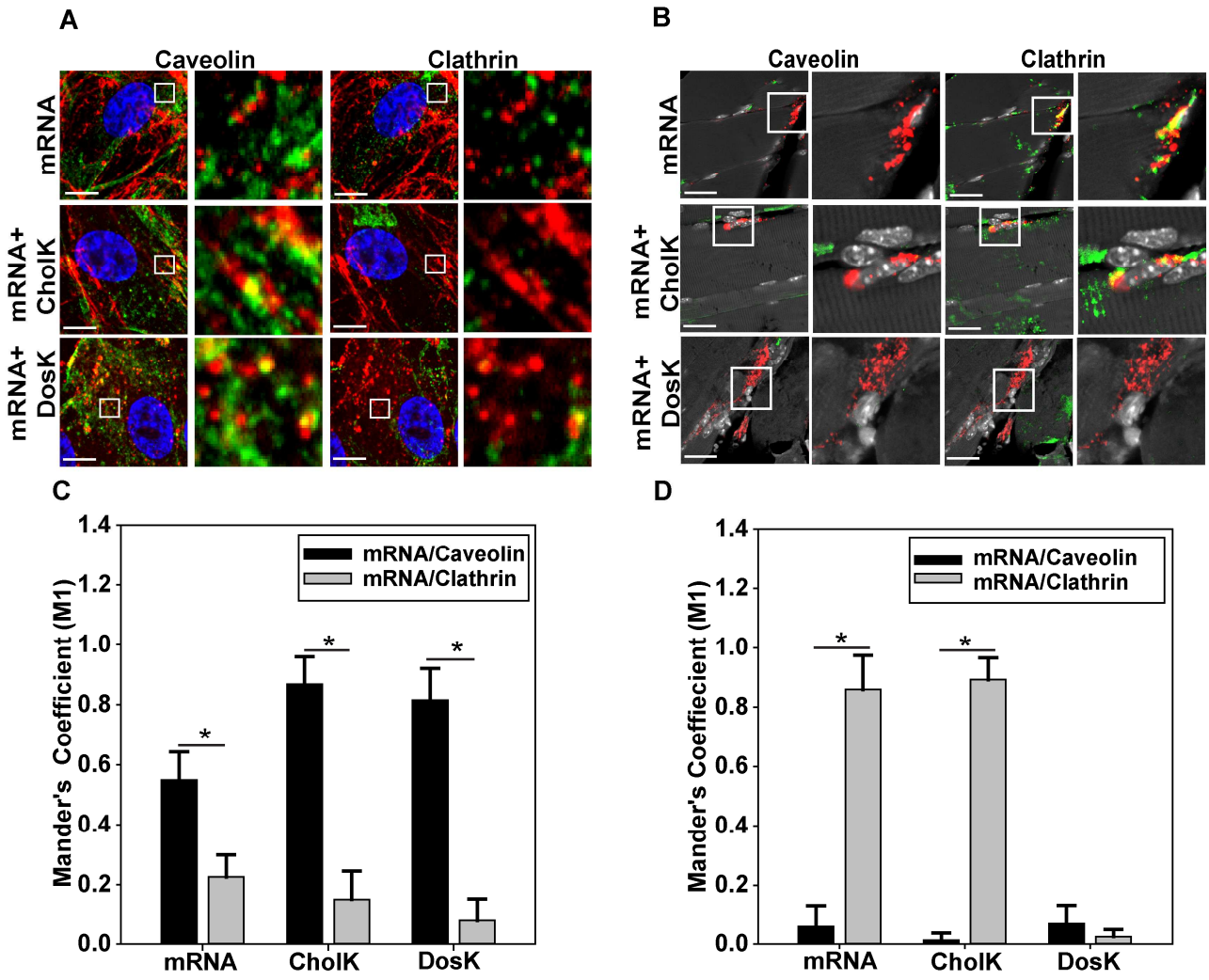

Fig. 2. IVT mRNA entry pathway differs *in vitro* and *in vivo.* A) mRNA colocalization with caveolin1 and Clathrin in HSkMSC cells transfected with 500 ng of mRNA alone and complexed with CholK or DosK 1.5 h post-delivery. Labeled mRNA is shown in red, the endosomal markers caveolin or clathrin in green and nuclei are stained with DAPI (blue). Scale bars are 15 µm. The experiment was performed three times in duplicate. B) Tissue sections from mice injected with 10µg of labeled-mRNA (red) alone and complexed with CholK or DosK in anterior tibialis muscle, i.m. Tissue sections were stained with caveolin and clathrin (green). Nuclei are shown in white. Experiments were performed in 4 mice per condition. Images were taken on an Elyra confocal microscope with 60Xobjective. Scale bars are 15 µm. Colocalisation of labeled mRNA with caveolin / clathrin *in vitro* (C) and *in vivo* (D) quantified with mander's overlap coefficient via Volocity software. Analysis was performed on 15 myofibers per condition. Data is presented as mean of Mander's correlation coefficient (M1) with SD. * Indicates $p<0.05$, tested by two-way ANOVA followed by Holm-Sidak multiple comparison testing.

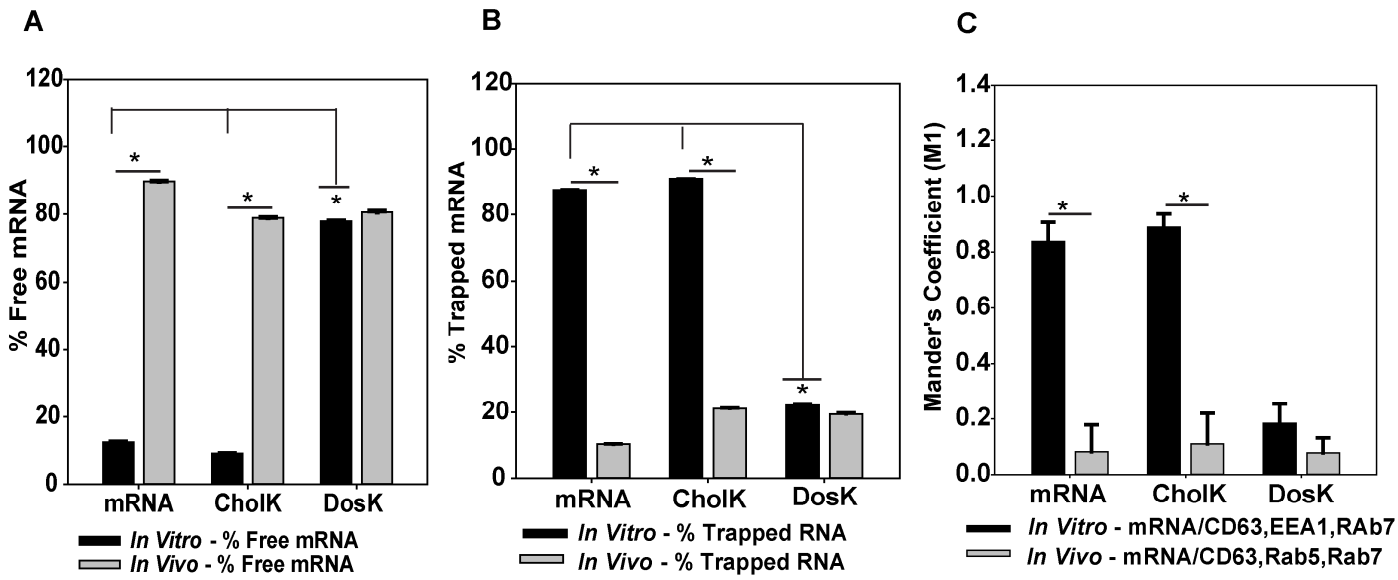

Fig. 3. IVT mRNA release from the endosomal system *in vitro* and *in vivo*. HSkMSC cells were transfected with 500 ng of mRNA alone or complexed with CholK or DosK and stained with early to late endosomal markers (CD63, EEA1 and Rab7) 6 h post-delivery. Mice (n=4) were injected with10 µg of labeled mRNA alone or complexed with CholK or DosK. Tissue sections from muscle tissue were extracted 6 h post-delivery and were stained with endosomal markers (CD63, Rab5 and Rab7). The mRNA release in *in vitro* and *in vivo* studies was quantified as the percentage of free (A) and endosome trapped mRNA (B). mRNA colocalization with endosomal markers was quantified by the Mander's overlap coefficient (C). Analysis was performed on 15 myofibers per condition. The experiment was repeated twice in duplicate. Statistically significant difference was tested by two-way ANOVA followed by Holm-Sidak multiple comparison; * Indicates $p<0.05$.

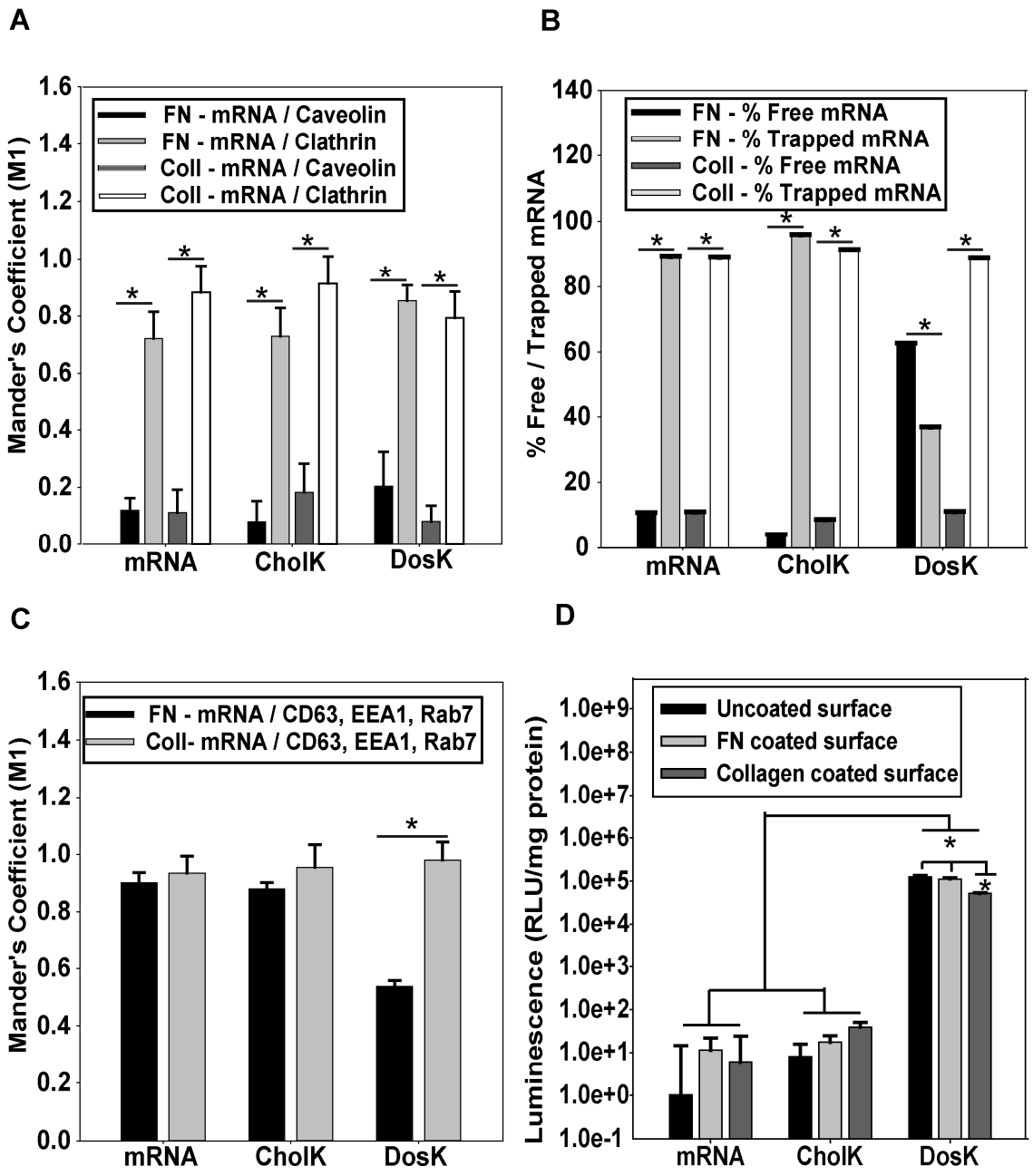

Fig. 4. Effect of ECM on mRNA entry, release and protein production. Colocalization of labeled IVT mRNA with A) Caveolin or clathrin or C) endosomal markers CD63, EEA1 and Rab7 quantified with Mander's overlap coefficient. B) mRNA released from late endosomes was quantified by calculating the percentage of free or trapped mRNA as described in material and methods. Quantification was performed on 15 myofibers per condition. The experiment was repeated twice in duplicate. D) HSkMSC cells were plated on untreated glass coverslips or coated with fibronectin and collagen and were transfected with 500 ng of mRNA alone or complexed with CholK or DosK. Luciferase activity was measured with the bright glo assay system 24 h post-delivery and the reads were normalized to untransfected controls. The mean luminescence was plotted as RLU per mg protein. * Indicates $p < 0.05$, tested by two-way ANOVA followed by Holm-Sidak multiple comparison.

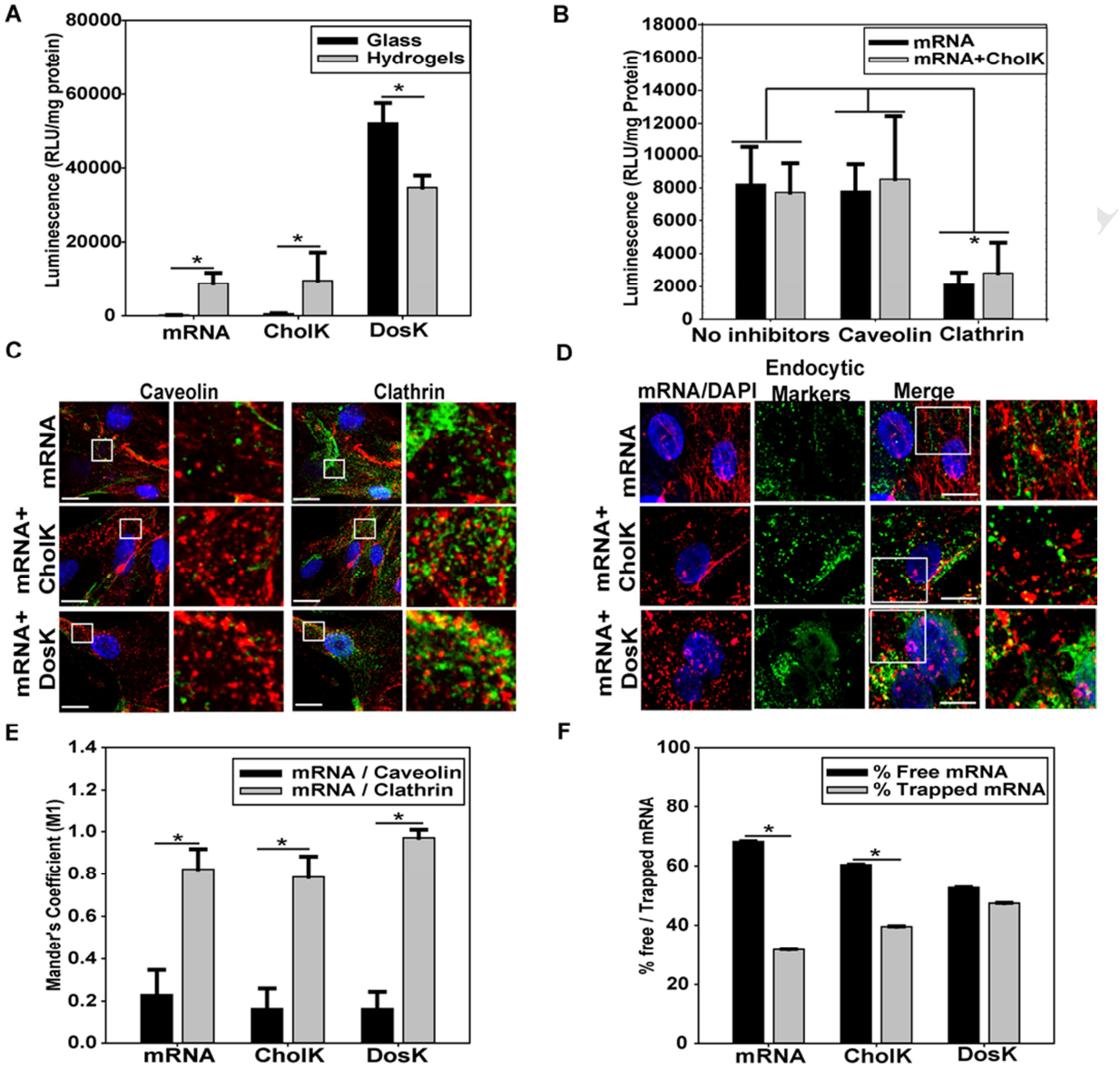

Fig. 5. Protein expression, mRNA endosomal entry and release in muscle cells plated on hydrogels. HSkMSC cells were seeded on 25 mm coverslips or on hydrogels. The next day, cells were transfected with 8 µg of IVT mRNA alone or complexed with CholK or DosK. A) Luciferase assay performed 24 h post transfection using the bright glo luciferase system and the reads were normalized to untransfected controls. B) HSkMSC were plated on glass coverslips or hydrogels and were treated with caveolin and clathrin inhibitors prior to mRNA transfection. The luciferase assay was performed 24 h post-delivery and the reads were normalized to untransfected controls. Statistically significant difference was tested by two-way ANOVA followed by Holm-Sidak multiple comparison, * Indicates $p<0.05$. Colocalization results between fluorescently labeled mRNA (red) and C) caveolin or clathrin (green) and D) with late endosomal markers (green). Scale bars are 15 µm. E) Quantification of colocalization with the mean Mander's overlap coefficient between mRNA and caveolin or clathrin. F) mRNA release is quantified as the average percentage of free and trapped mRNA. Analysis performed on 15 myofibers per condition. The experiment was repeated twice in duplicate. * Indicates $p<0.05$, tested by two-way ANOVA followed by Holm-Sidak multiple comparison.

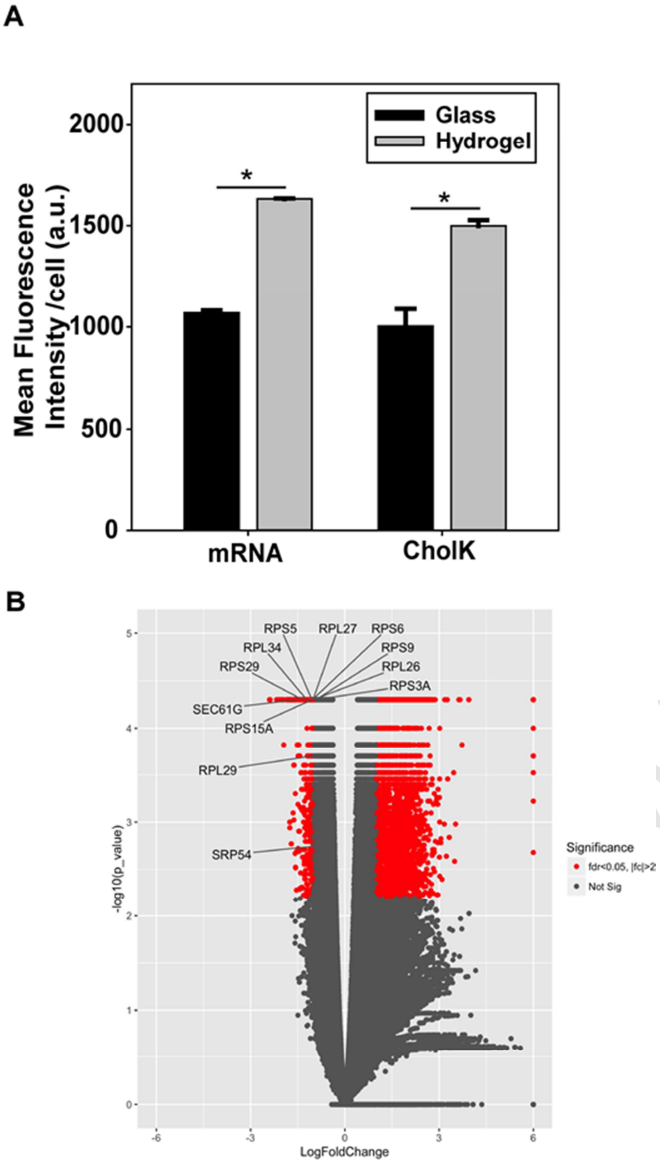

Fig. 6. Factors associated with efficient translation of mRNA on Hydrogels. A) Uptake of IVT mRNA upon delivery to cells plated on glass versus hydrogels. HSkMSC cells were plated on glass coverslips or hydrogels and were transfected with 8 µg of mRNA alone or complexed with CholK. The mean mRNA fluorescence intensity per cell was measured by flow cytometry and analyzed with the Flow Jo software. B) Total RNA was isolated from muscle cells seeded on glass coverslips and hydrogels and RNA sequencing was performed on cells plated in triplicate. Volcano plot indicating in red the genes that are significantly expressed by cells cultured on hydrogels as compared to glass coverslips.

Table 1: Translational efficiency of nanocomplexes *in vitro* and *in vivo.*

Nanocomplexes	***In vitro***	***In vivo***
(Aminoethyl)chitin/ DNA [11]	2.5-fold increase in transfection efficiency and lower toxicity than naked DNA	NA
Lipopeptide with optimal histidine and lysine [12]	High stability and efficient transfection	NA
DOTAP based cationic liposomes [13]	Efficient Delivery of siRNA to lung cells	NA
DOTMA based cationic liposomes [13]	Increased cellular delivery of siRNA to human airway epithelial cells and mouse neuroblastoma cells	NA
Ethylphosphocholine based lipoplexes [13]	Low cytotoxity	Highest intrapulmonary delivery for lung cancer therapy
Cationic lipid dioctadecylamido glycylspermine (Transfectam, DOGS) [14]	NA	High level of transfection in mouse brain
Cholesterol based nanoplexes [15]	Efficient transfection in presence of NaCl	Efficient transfection in water with respect to naked DNA
Polyethylenimine, PEI / DNA complexes [16]	Low transfection efficiency	High transfection efficiency
Pegylated DOTAP/Cholesterol – DNA complexes [17]	Inefficient transfection	Improved stability and biodistribution
Nonionic amphiphile block copolymer PE6400/DNA complexes[18]	Inefficient transfection	High transfection efficiency in skeletal and cardiac muscles

Table 2: Sequence of the oligonucleotides targeting the 3'UTR region of the IVT mRNA.

RNA target	Sequences
Homo sapiens albumin (ALB) mRNA (3' UTR), NM_000477.6	GCATCACATTTAAAAGCATCTCAGCCTACCATGAGAATAAGA GAAAGAAAATGAAGATCAATAGCTTATTCATCTCTTTTTCTTT TTCGTTGGTGTAAAGCCAACACCCTGTCTAAAAAACATAAATT TCTTTAATCATTTTGCCTCTTTTCTCTGTGCTTCAATTAATAAA AAATGGAAA
Probe 1	TTTXTTT**UAXUCUCAXGGUAGGCXGA**
Probe 2	TTTXTTT**GAXGAAUAAGCXAUUGA**
Probe 3	TTTXTTT**ACAGGGXGUUGGCXUUACA**
HBA1 – Homo sapiens hemoglobin subunit alpha 1 mRNA (3' UTR), NM_000558.4	GCTGGAGCCTCGGTGGCCATGCTTCTTGCCCCTTGGGCC TCCCCCCAGCCCCTCCTCCCCTTCCTGCACCCGTACCCCC GTGGTCTTTGAATAAAGTCTGAGTGGGCGGCAAAAAAAAA AA
Probe 1	TTTTTTT**AAGCAUGGCCACCGAGG**
Probe 2	TTTTTTT**UCAAAGACCACGGGGG**
Probe 3	TTTTTTT**GCCGCCCACUCAGACU**
	Boldface: 2'-O-Methyl RNA; X: dT-C6-NH2; all others are DNA; underline: binding region

Table 3: Result of GSEA analysis.

Pathway name	P value
Kegg Ribosome	0
mRNA Translation	0
Metabolism of mRNA Translation	0
3' UTR Mediated mRNA Translation	0

Four pathways identified by the GSEA method related to mRNA translation are enriched in cells transfected on hydrogel. P values are indicated.

Table 4: List of genes related to RNA translation pathways.

GENE SYMBOL	GENE_TITLE	RANK IN GENE LIST	RANK METRIC SCORE	RUNNING ES	CORE ENRICHMENT
SRP54	signal recognition particle 54kDa	2500	1.01	-0.2915	Yes
RPL26	ribosomal protein L26	2528	-1.009	-0.2726	Yes
RPS6	ribosomal protein S6	2570	-1.029	-0.2579	Yes
RPL27	ribosomal protein L27	2582	-1.034	-0.2327	Yes
RPL29	ribosomal protein L29	2588	-1.037	-0.2054	Yes
RPS15A	ribosomal protein S15a	2594	-1.041	-0.178	Yes
RPS9	ribosomal protein S9	2602	-1.044	-0.1511	Yes
RPS5	ribosomal protein S5	2605	-1.044	-0.1226	Yes
RPL39	ribosomal protein L39	2788	-1.206	-0.1517	Yes
RPL34	ribosomal protein L34	2793	-1.214	-0.119	Yes
EIF3E	Translational Initiation Factor 3	2799	-1.218	-0.0866	Yes
RPS29	ribosomal protein S29	2852	-1.349	-0.0668	Yes
SEC61G	Sec61 gamma subunit	2886	-1.544	-0.0349	Yes
RPS3A	ribosomal protein S3A	2902	-1.653	0.0062	Yes

Genes overexpressed in cells transfected on hydrogels and enriched in the RNA translation and 3'UTR mediated RNA translation pathways.

Table 5: Summary of experimental results.

	In vitro	***In vivo***	**Hydrogel**
Naked mRNA	No protein expression	High protein expression	Higher protein expression than *in vitro*
	Caveolin-mediated endocytosis	clathrin-mediated endocytosis	clathrin-mediated endocytosis
	mRNA trapped in endosomes 6h post delivery	mRNA released from endosomes 6h post delivery	mRNA released from endosomes 6h post delivery
mRNA+ CholK	No protein expression	High protein expression	Higher protein expression than *in vitro*
	Caveolin-mediated endocytosis	clathrin-mediated endocytosis	clathrin-mediated endocytosis
	mRNA trapped in endosomes 6h post delivery	mRNA released from endosomes 6h post delivery	mRNA released from endosomes 6h post delivery
mRNA+ DosK	High protein expression	No protein expression	Lower protein expression than *in vitro*
	Caveolin-mediated endocytosis	No mRNA entry	clathrin-mediated endocytosis
	mRNA released from endosomes 6h post delivery	NA	mRNA released from endosomes 6h post delivery

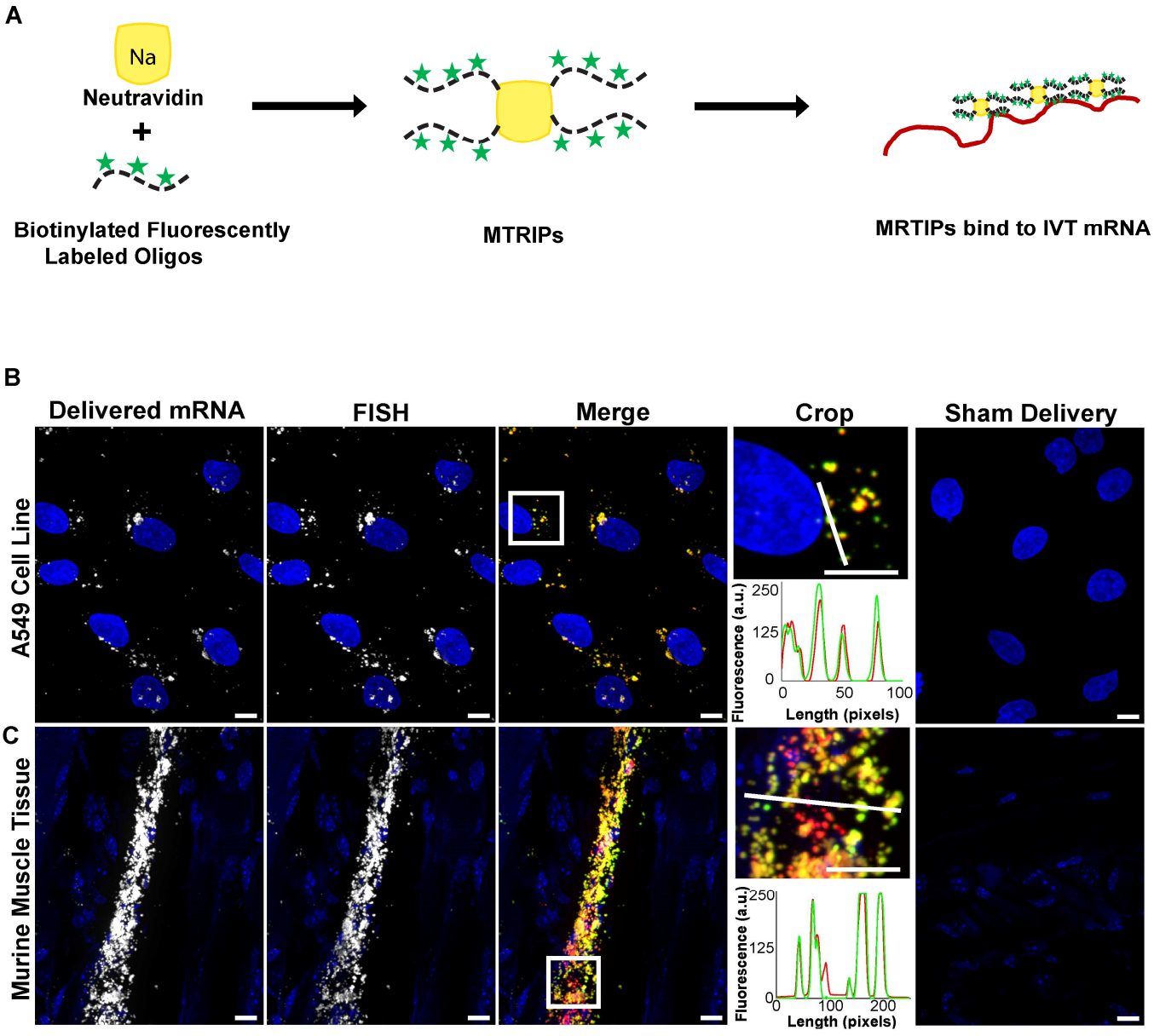

Fig. S1. Schematic of IVT mRNA labeling and FISH. A) Neutravidin (yellow) is conjugated to biotinylated fluorescently labeled (green stars) oligonucleotides (black dotted line) to form MTRIPs. Three MTRIPs complementary to three sequences within the 3'UTR of the IVT mRNA are utilized for labeling and visualization *in vivo* and *in vitro*. B) Dylight 650 pre-labeled mRNA (100 ng) were delivered to A549 cells using Viromer RED-based transfection. Six hours after delivery, cells were fixed and FISH was performed using 5nM Quazar 570 Stellaris RNA probes complementary to the transcript coding region. The colocalization of the MTRIP (red) and FISH (green) fluorescent signals is demonstrated by the intensity profile along the white line in the cropped image corresponding to the boxed area. C) Cy3b pre-labeled mRNA (10 µg) were delivered to mice via IM injection. Two hours after delivery, mice were sacrificed and tissue samples utilized for FISH with 5 nM Quazar 670 Stellaris RNA probes complementary to the transcript coding region. The colocalization of the MTRIP (red) and FISH (green) fluorescent signals is demonstrated by the intensity profile along the white line in the cropped image corresponding to the boxed area. No fluorescence signal is observed in mock transfected cells (sham delivery).

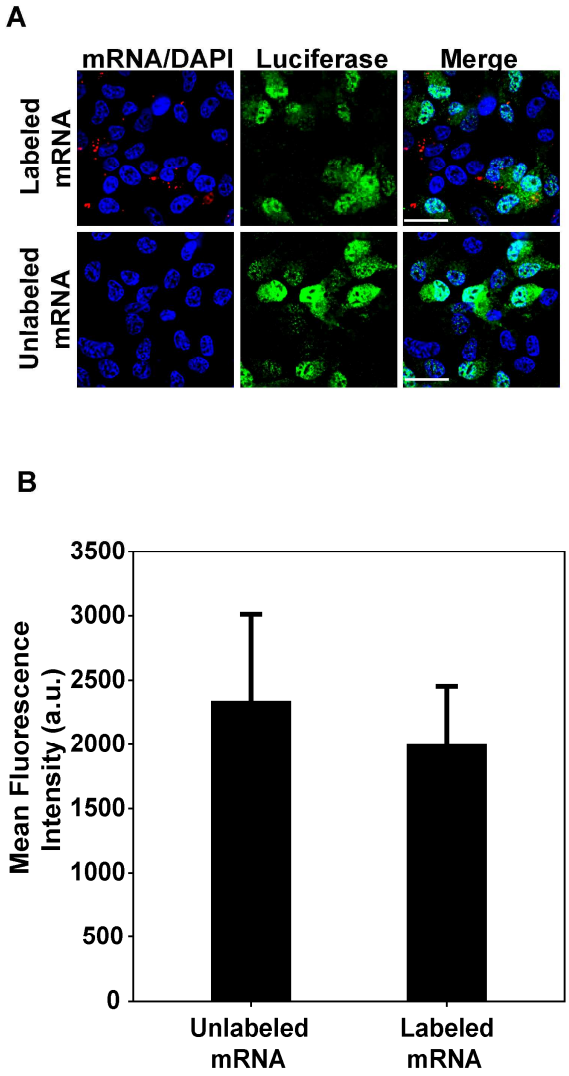

Fig. S2. Characterization of IVT mRNA labeling. A) Luciferase expression in HeLa cells was measured in cells transfected with Lipofectamine 2000 with 300ng of unlabeled or Cy3 labeled mRNA. Labeled mRNA is shown in red, luciferase protein expression in green and nuclei stained with DAPI in blue. The scale bars are 15 µm. B) Quantification was performed on 30 cells and mean fluorescence intensity was plotted. The experiment was repeated twice in duplicate.

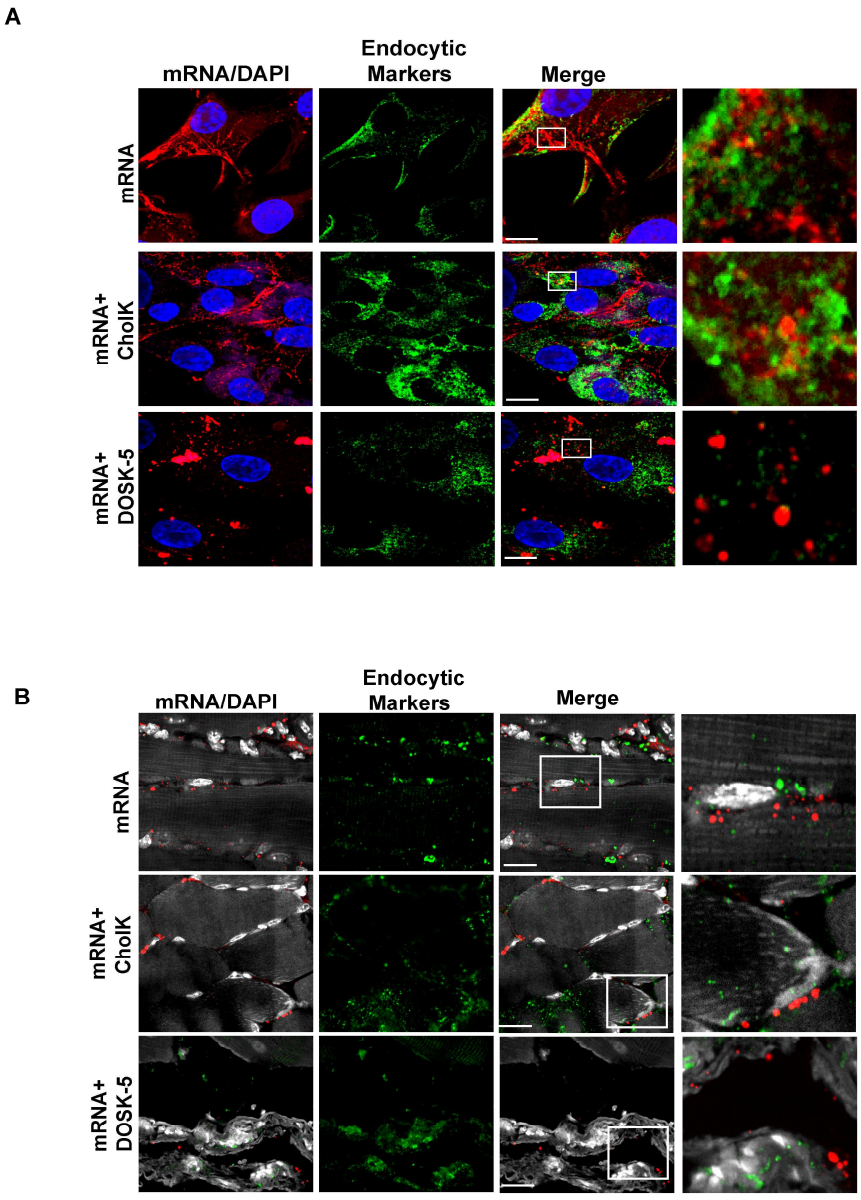

Fig. S3. IVT mRNA endosomal release *in vitro* and *in vivo*. A) HSkMSC cells were transfected with 500 ng of mRNA alone or complexed with CholK or DosK and stained with early to late endosomal markers (CD63, EEA1 and Rab7) 6h post delivery. The labeled RNA is shown in red, endosomal markers in green and nuclei in blue. The experiment was performed three times in duplicate. B) Mice (n=4) were injected with10 µg of labeled mRNA alone or complexed with CholK or DosK. Tissue sections from muscle tissue were extracted 6 h post delivery and were stained with endosomal markers (CD63, Rab5 and Rab7). Representative images show mRNA in red, endosomal markers in green and nuclei in white. Scale bars are 15 µm.

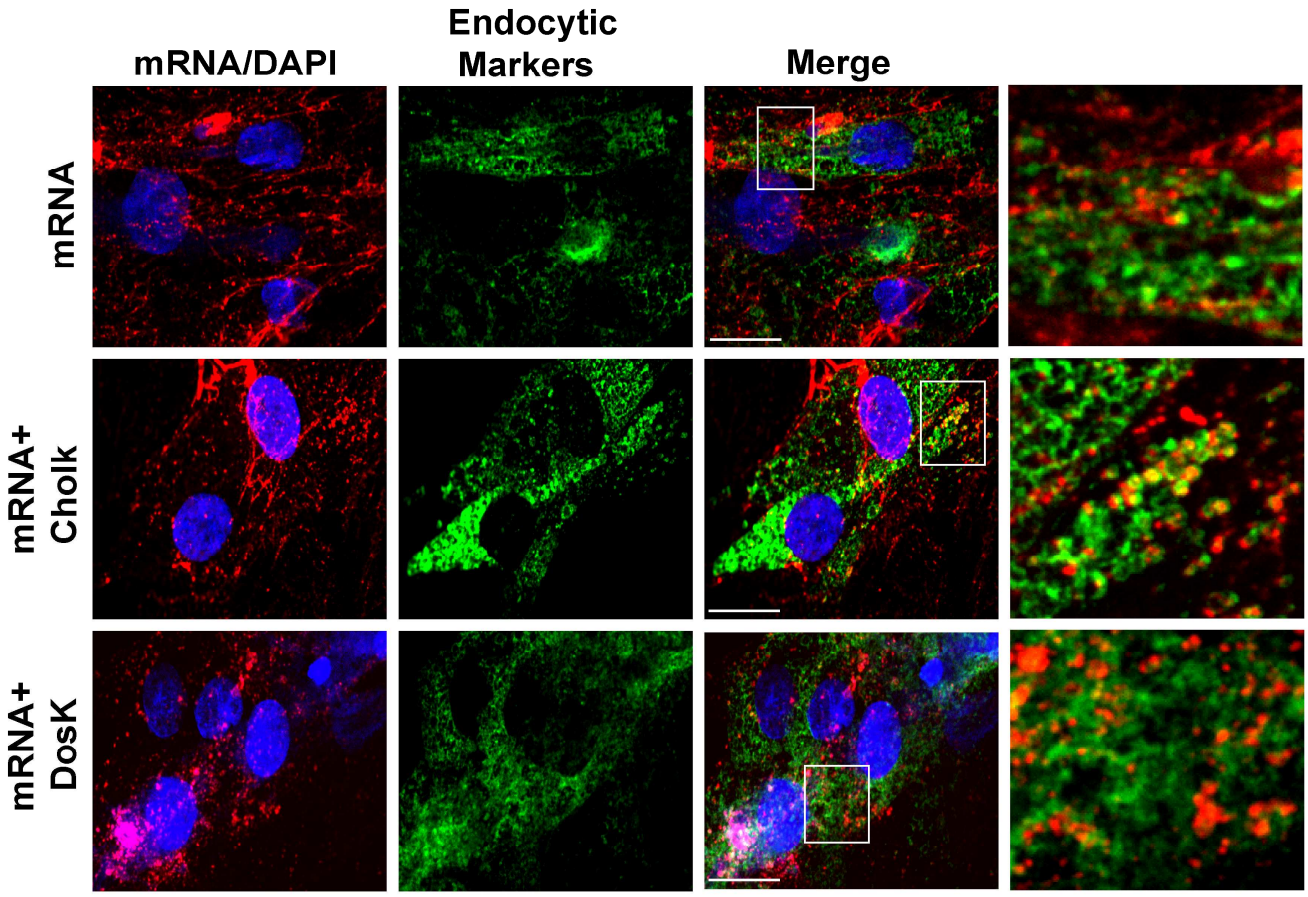

Fig. S4. Immunofluorescence for Late endosomal markers *in vitro.* HSkMSC cells were transfected with 500 ng of IVT mRNA alone or complexed with CholK or DosK and stained with early to late endosomal markers (CD63, EEA1 and Rab7) 1.5h post-delivery. Labeled mRNA is shown in red, endosomal markers in green and nuclei in blue. Scale bars are 15 µm. Experiment was performed independently twice in duplicate.

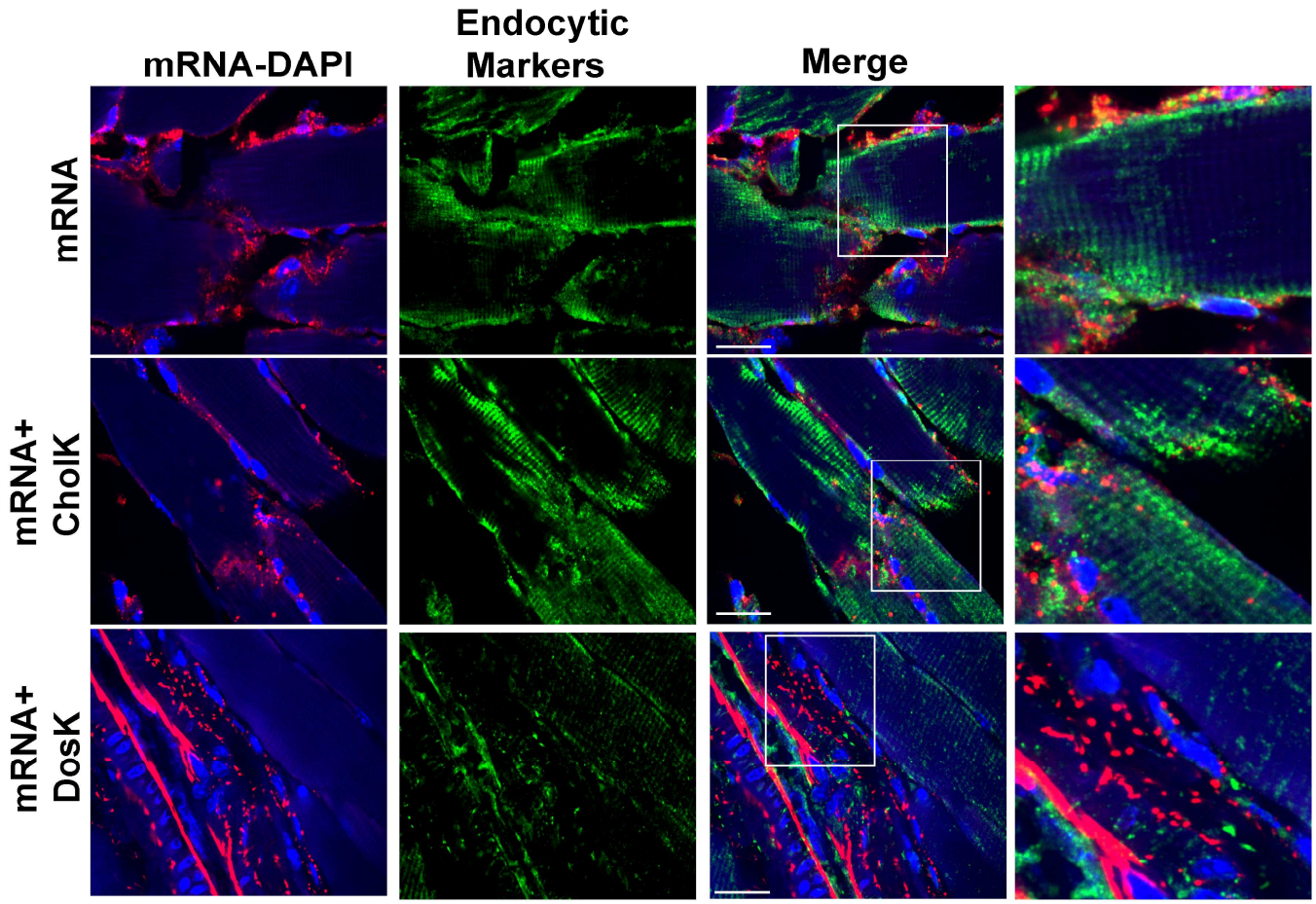

Fig. S5. Immunofluorescence for endosomal markers *in vivo.* Mice (n=4) were injected with 10 µg of labeled IVT mRNA alone or complexed with CholK or DosK. Tissue sections from muscle tissue were extracted 1.5h post delivery and were stained with endosomal markers (CD63, Rab5 and Rab7). Representative images show mRNA in red, endosomal markers in green and nuclei in blue. Scale bars are 15 µm.

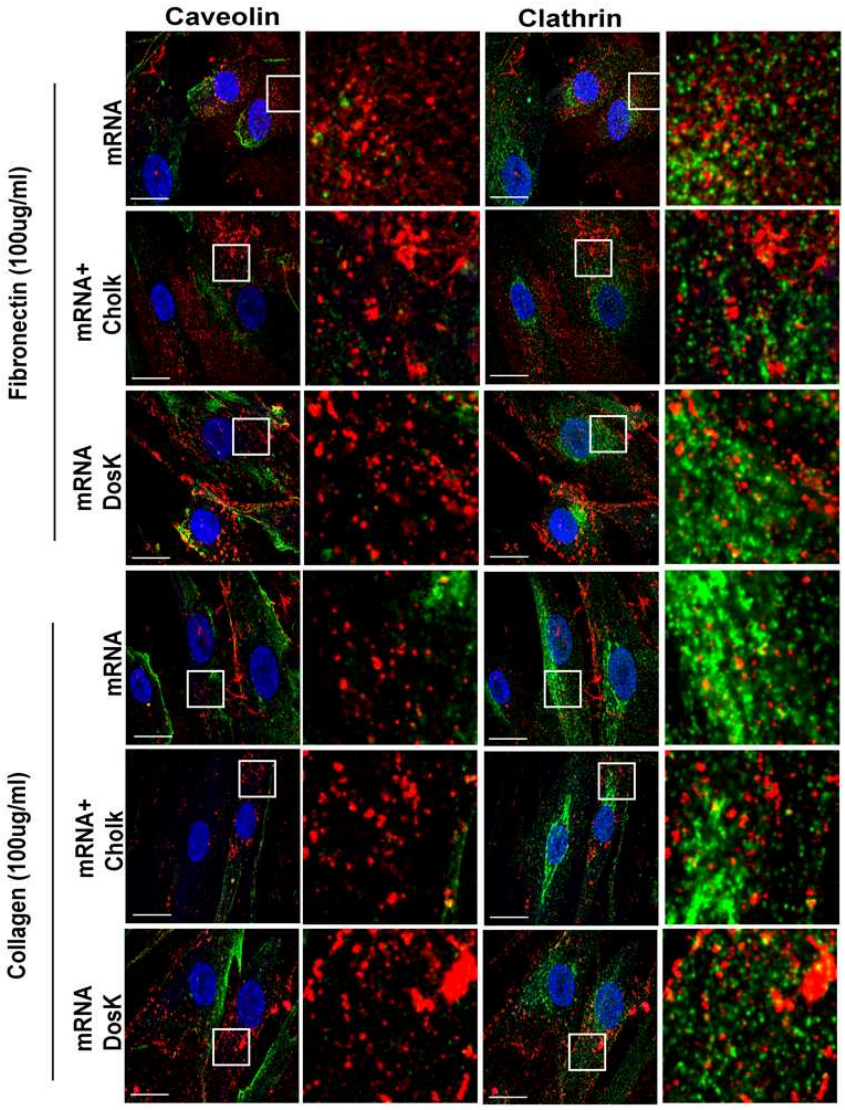

Fig. S6. Effect of ECM proteins on IVT mRNA endocytic pathway. HSkMSC cells were grown on Labtek II plates coated with fibronectin and collagen (100 µM) and were transfected with 500 ng of cy3b labeled mRNA (red) alone or complexed with CholK or DosK. Cells were stained with endosomal entry markers caveolin1 and clathrin (green) 1.5h post delivery. The experiment was performed thrice in duplicate.

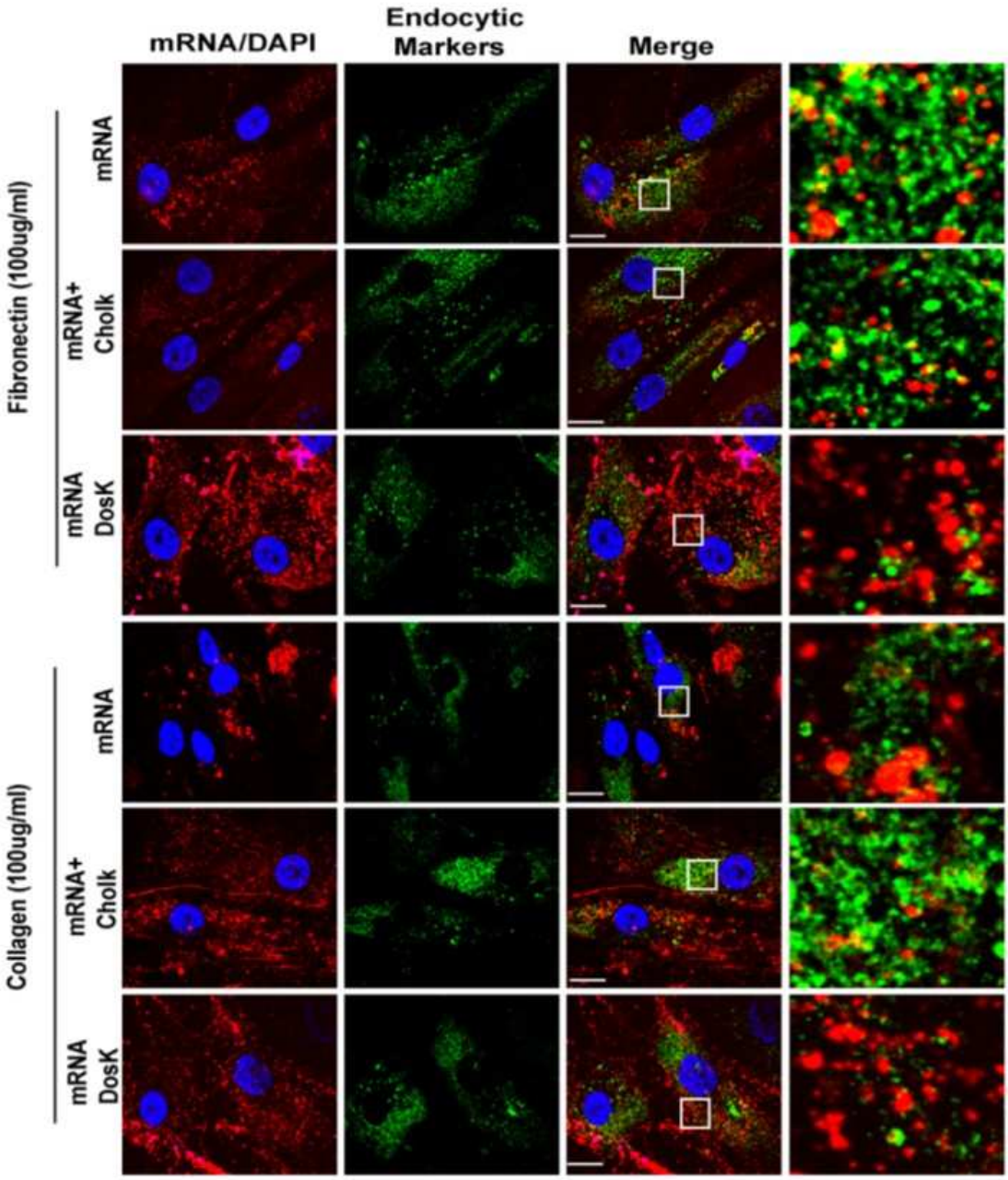

Fig. S7. Effect of ECM proteins on IVT mRNA endosomal release. Cells were stained with mid to late endosomal markers, CD63, EEA1 and Rab7, 6h post delivery. Labeled mRNA is shown in red, endosomal entry markers or mid to late endosomal markers in green and nuclei in blue. Scale bars are 15 μm. Experiment was performed three times in duplicate.

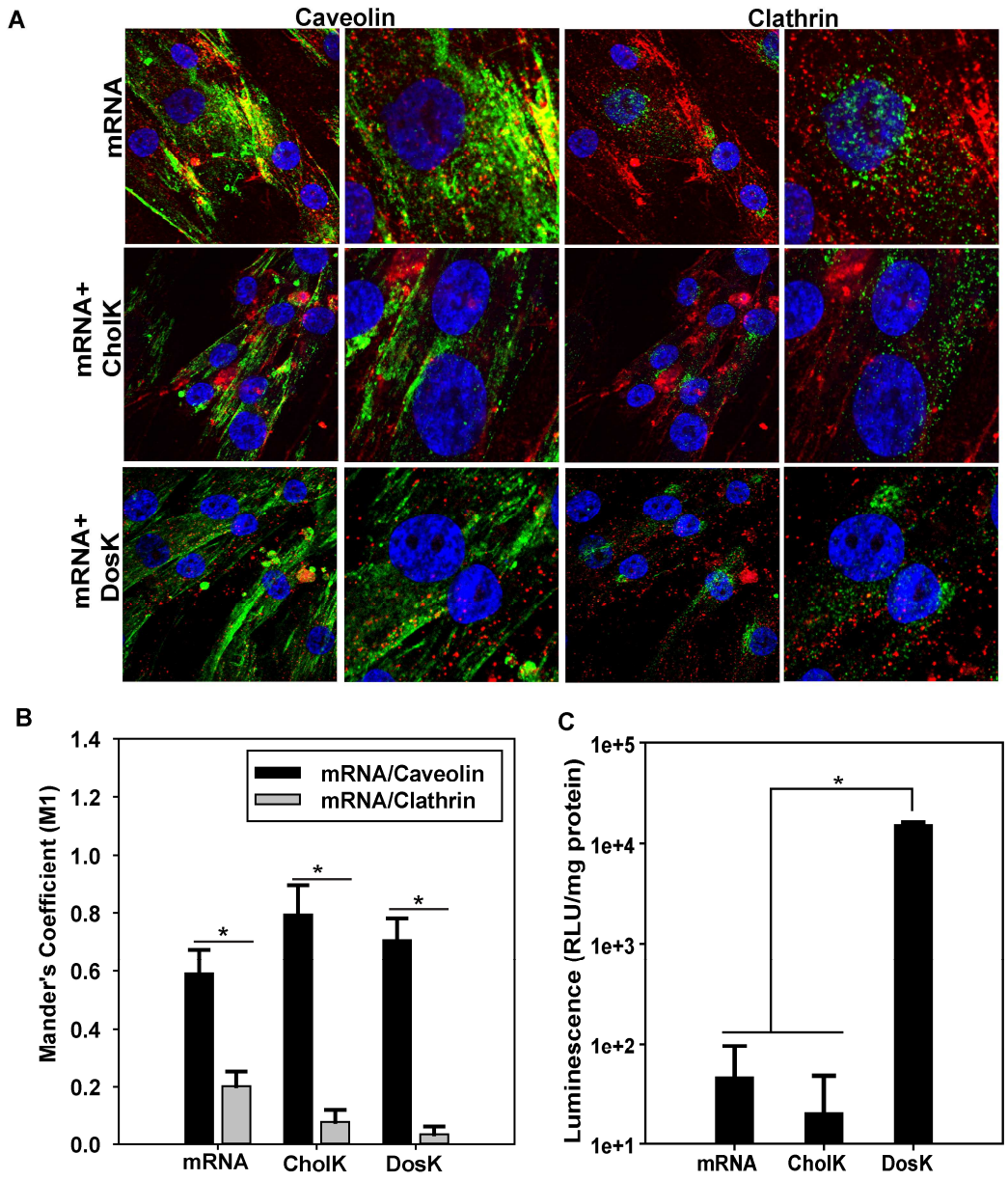

Fig. S8. IVT mRNA entry pathway and protein expression in differentiated myotubes. A) mRNA colocalization with caveolin1 and clathrin in myotubes transfected with 500 ng of mRNA alone and complexed with CholK or DosK 1.5h post-delivery. Labeled mRNA is shown in red, the endosomal markers caveolin or clathrin in green and nuclei are stained with DAPI (blue). Scale bars are 15 µm. The experiment was performed twice in duplicate. B) Colocalization of labeled mRNA with caveolin / clathrin *in vitro* was quantified with mander's overlap coefficient via Volocity software. Analysis was performed on 20 myofibers per condition. Data is presented as mean of Mander's correlation coefficient (M1) with SD. * Indicates $p<0.05$, tested by two-way ANOVA followed by Holm-Sidak multiple comparison testing. C) The Luciferase activity was detected by bright glo luciferase assay system and the reads were normalized to untransfected controls. * Indicates $p<0.05$, tested by one-way ANOVA followed by Holm-Sidak multiple comparison testing**.** The experiment was performed twice in triplicate.

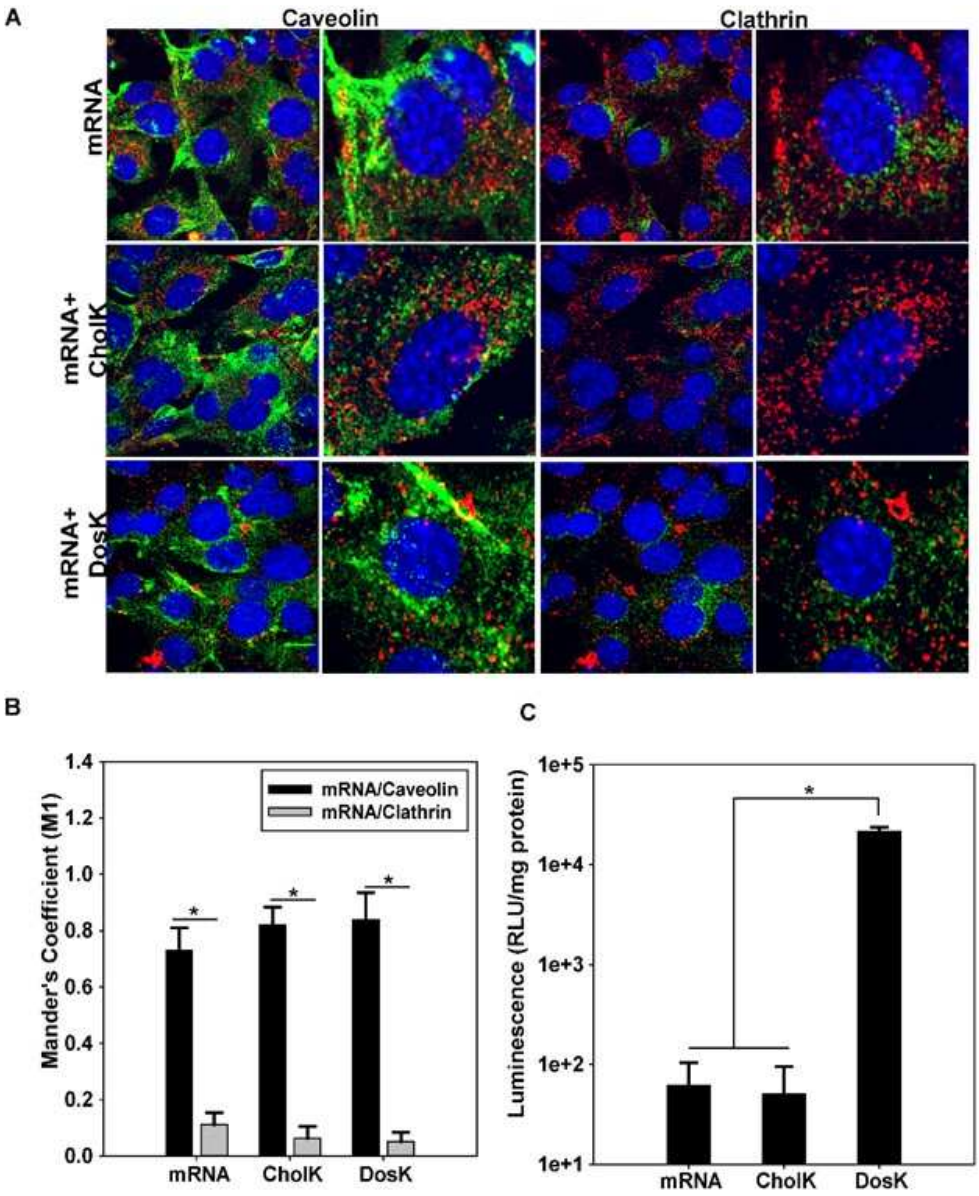

Fig. S9. IVT mRNA entry pathway and protein expression of IVT mRNA in Sol8. A) mRNA colocalization with caveolin1 and clathrin in mouse muscle cells transfected with 500 ng of mRNA alone and complexed with CholK or DosK 1.5h post-delivery. Labeled mRNA is shown in red, the endosomal markers caveolin or clathrin in green and nuclei are stained with DAPI (blue). Scale bars are 15 µm. The experiment was repeated once in duplicate. B) Colocalization of labeled mRNA with caveolin / clathrin *in vitro* was quantified with mander's overlap coefficient via Volocity software. Analysis was performed on 20 cells per condition. Data is presented as mean of Mander's correlation coefficient (M1) with SD. * Indicates $p<0.05$, tested by two-way ANOVA followed by Holm-Sidak multiple comparison testing. C) The Luciferase activity was detected by bright glo luciferase assay system and the reads were normalized to untransfected controls. * Indicates $p<0.05$, tested by one-way ANOVA followed by Holm-Sidak multiple comparison testing**.** The luciferase assay was performed twice in triplicate.

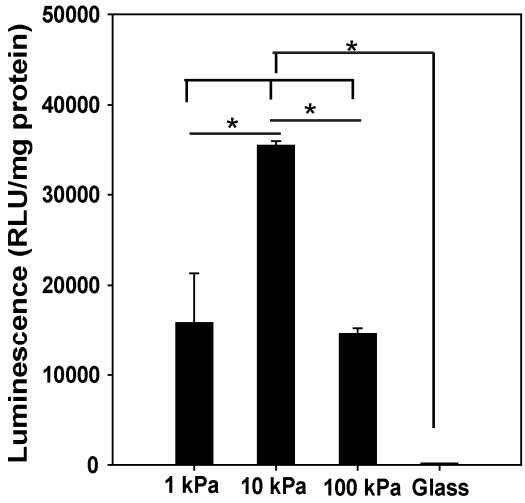

Fig. 10. Protein expression on human skeletal muscle cell line plated on varying substrate stiffness. HSkMSC cells were seeded on 25 mm coverslips or on hydrogels of varying stiffness (1, 10 and 100 kPa) as well as on glass. The next day, cells were transfected with 8 µg of mRNA complexed with CholK. Luciferase assay was performed 24 h post transfection using the bright glo luciferase system and the reads were normalized to untransfected controls. * Indicates $p<0.05$, tested by one-way ANOVA followed by Holm-Sidak multiple comparison testing**.** The luciferase assay was performed twice in triplicate.

.